J. theor. Biol. (1989) **138,** 353–405

Electrical Instability in Cardiac Muscle: Phase Singularities and Rotors

A. T. WINFREE

University of Arizona, Tucson, Arizona 85721, *U.S.A.*

(*Received* 27 *October* 1988, *and accepted in revised form* 10 *February* 1989)

A dynamical system is "excitable" at some stage in its behavior (e.g. at a rest state or while it is nearly at rest prior to a spontaneous event) if a small, but not too small, stimulus of the right kind elicits an immediate big reaction that eventually leads back to the original state. During this return to excitability a typical system is not excitable. An excitable system need not have an attracting rest state; a spontaneous oscillator can be excitable, too, as is common in biological and in chemical excitable kinetics.

In a medium characterized by such excitable dynamics at every point, the excitation can propagate as a travelling pulse. Undamaged cardiac muscle shares with other excitable media certain features of such pulse propagation in two and three dimensions. Among the new electrophysiological phenomena thus anticipated are paired mirror-image vortices ("rotors") organized around phase singularities. These should arise in the myocardium near the intersection of a moving critical contour of phase in the normal cycle of excitation and recovery with a momentary critical contour of local stimulus strength. Such intersections, and the corresponding aftermath of paired rotors, should only occur following certain combinations of stimulus size and stimulus timing. Plotting those combinations on a "vulnerability diagram", one delineates a domain for creation of rotors (corresponding to tachycardia) surrounded on all sides by a halo of combinations at which just a few repetitive responses follow stimulation. The experiments called for to check these implications have now been carried out in the special case of electrically-induced tachycardia in healthy canine ventricle. They support the two-dimensional theory, so a new experiment is suggested to demonstrate wholly intramural three-dimensional vortex filaments.

1. Introduction

During the 1970's, many investigators independently improved on early models of cardiac re-entry in overly idealized excitable media by attempting numerical simulations involving more than one local state variable, a more realistic coupling mechanism, and finer spatial discretization (e.g. Gul'ko & Petrov, 1972; Shcherbunov *et al.*, 1973; Winfree, 1973, 1974*a*,*b*, 1978; van Capelle & Durrer, 1980). The fundamental features of vulnerability to re-entrant tachycardia on the scale of 10 mm and up ("macro-reentry") turned out to be latent even in cable-equation models which ignore such significant features as damage by infarcts, the conspicuous anisotropy of undamaged cardiac muscle, and the discreteness of its cell-to-cell coupling on the 10–100 μ scale. Such models resolved for the first time the electrophysiological

0022-5193/89/110353+53 $03.00/0

dynamics of the vortex center of reentrant action potentials, at least in ideally continuous media. Adequately detailed comparison with intracellular recordings from actual cellular media still remains a technical challenge.

These interpretations of reentry have an intuitive, but unfamiliar, geometrical representation in terms of the spatial distribution of two membrane properties that change during passage of an action potential: local membrane potential or degree of excitation, and a "recovery process" which, together with local membrane potential, governs local refractoriness. They can also be simplified even more to a geographical description in terms of a single variable, the local phase in the repeated cycle of excitation and recovery that the myocardium experiences during normal sinus rhythm or during periodic drive by a ventricular tachycardia. In these terms, the locus from which re-entrant waves radiate (the edge of the vortex) is associated with a "phase singularity" (the wave's pivot point; see section 2 below) in the simplified model. The logic of phase singularities makes it peculiarly easy to anticipate several surprising consequences of the basic idea that myocardium is a typical excitable medium. Experimental protocols were suggested by which these phenomena might be sought (Winfree, 1983, 1986*b*, 1987). They have since been sought and found (Ideker & Shibata, 1986; Chen *et al.*, 1988; Frazier *et al.*, 1988*b*; Shibata *et al.*, 1988, Frazier *et al.*, 1989).

The purpose of this paper is to review the theoretical basis of those inferences/predictions in a more quantitative way by reverting to their origin in simple numerical models and numerically implementing the "pinwheel experiment" using the FitzHugh–Nagumo model (see below) scaled for application to ventricular myocardium. This application was originally executed only as an unpublished cross-check on the more abstract and idealized line of reasoning about phase and phase singularities, then in press (Winfree, 1987). It was intended as the prototype of a more exact calculation based on the most recent quantitative understanding of cardiac membrane electrophysiology. But the stimulation protocol applied in the model has since been executed in canine ventricle, with strikingly similar results. And the more explicitly channel-oriented electrophysiological models have turned out not to fit the experimental results after all, until adjusted like the simpler models with appropriate "fudge factors". So it is time to present the "prototype".

The remainder of this paper is organized as follows. Section 2 reviews in many paragraphs the concepts alluded to by more compact jargon words and phrases in this field; many readers will want to proceed directly to section 3. Section 3 describes the impact of a geographically graded premature stimulus on an excitable medium in which the timing of excitation and recovery is also geographically graded: initial conditions are created which can then evolve into vortex-like action potentials. In section 4 this conceptual scheme is implemented numerically, using the FitzHugh–Nagumo membrane model in a setting (the "pinwheel experiment") that suggests implementation in cardiac muscle. The Beeler–Reuter model of ventricular muscle is shown to support vortices similar to those seen in simpler models. Section 5 briefly summarizes the results of recent experimental work along similar lines. A short conclusion in section 6 calls attention to the next necessary experi-

ment. The Appendix contains background and detail about the numerical implementations.

2. Terminology

Before examining the model and its implications, it may be helpful to clarify some vocabulary: tachycardia, reentry, vulnerability, vulnerable period, fibrillation, epicardial map, isochrons, phase singularity, arrhythmia or dysrhythmia, critical phase, vortex and rotor.

Tachycardia just means a "quicker heartbeat" than whatever is normal at rest. In man the clinical definition implies beat-to-beat intervals of 600 msec or less; a typical ventricular tachycardia has a period of 200–400 msec. The mechanism of many tachycardias is reentry.

Reentry means reactivation of a patch of tissue by an action potential that returned without ever dying out. It was originally thought of in a one-dimensional context as a pulse circulating on a closed ring of cardiac fibers (as in Wolff-Parkinson-White syndrome) (Mines, 1914; Garrey, 1914). In recent decades the same idea has been applied to a two- or three-dimensional meshwork of connected fibers (the "wandering wavelets" model of Moe *et al.*, 1964, the "compound re-entry" associated with severely infarcted tissue, Mehra, 1984; Swenne *et al.*, 1986). We attempt to understand reentrant tachycardia in normal tissue not in terms of a source along one or several one-dimensional paths embedded within the thicker bulk, but in terms of fully two- and three-dimensional conduction (as in Gul'ko & Petrov, 1972; Shcherbunov *et al.*, 1973; Foy, 1974; Allessie *et al.*, 1977; van Capelle & Janse, 1980; Zykov, 1984; Mehra, 1984; Swenne *et al.*, 1986).

Vulnerability refers to the susceptibility of myocardium to a stimulus that switches it (commonly through a stage of reentrant tachycardia) from its usual slow rhythm of relatively synchronous contraction to a high-frequency, initially synchronous, but eventually asynchronous, mode called fibrillation. Some forms of reentrant ventricular tachycardia may persist stably without degenerating to fibrillation (as is the case in the atria) if circulation is artificially maintained, so it might become necessary to distinguish ventricular vulnerability to reentry from vulnerability to fibrillation. For present purposes, I mean vulnerability to vortex-like reentrant ventricular tachycardia, noting that this is commonly the onset of ventricular fibrillation; the mechanism of transition from such tachycardia to fibrillation is not known, nor is ventricular fibrillation understood.

Vulnerable Period refers to the interval of time during the cardiac cycle during which a momentary stimulus (e.g. an extracellular current) can instigate ventricular tachycardia (which commonly progresses spontaneously to fibrillation). The width of this interval depends on stimulus current and duration. This current need be only a few times stronger than the threshold required to evoke a propagating response somewhere in the heart using the same electrode configuration at the same time. The width of this interval is roughly the same as the time required for activation

(or recovery) to propagate completely through the ventricles. (There is also an atrial vulnerable period, to which the same concepts presumably apply, but here we focus exclusively on the ventricles.)

Fibrillation sounds like something about fibrils, and that is indeed the classical understanding: during fibrillation the cardiac muscle was originally imagined to function independently in its constituent fibrils, all twitching asynchronously. Such behavior in a discrete-state, geographically discontinuous medium was studied by Moe and co-workers (Moe, 1962; Moe *et al.*, 1964) as a model of atrial fibrillation. Pursuing Moe's analogy of fibrillation to hydrodynamic turbulence, Ruelle (1980) and Smith & Cohen (1984) have suggested that such fine-grained irregular dynamics may be understandable in terms of chaos and strange attractors. Although such may be the terminal condition after development of anoxia and ischemia secondary to circulatory failure, it might not provide a useful understanding of the earlier stages in normal tissue addressed here. During early stages, fibrillation or its immediate antecedent states are strikingly rhythmic (at an abnormally high frequency) (citations in Winfree, 1987, p.108 and 112; Goldberger *et al.*, 1986; Goldberger & Rigney 1989). If an additional stimulus is needed to induce transition from tachycardia into fibrillation, then this analysis concerns only the induction of tachycardia. But if the transition is spontaneous then tachycardia is the first stage, the onset of fibrillation. It is not known what happens during the transition, though it has long been thought to entail microscopic disorder born of the discretely different properties of adjacent fibers. Multi-electrode recorders capable of providing an answer have recently been constructed in several laboratories.

In this article we consider (an interpretation of) just the *onset* of fibrillation in the form of macro-reentrant tachycardia in the normal healthy mammalian ventricle, thought of as a continuum on the pertinent scales of time and space.

Epicardial maps and isochron(e)s: during the onset of ventricular fibrillation a short-period cycle (about 100 msec in dogs, about twice that in humans) dominates the whole ventricle, so every point in the ventricle can be assigned some phase in this cycle. The geographical distribution of phase is a kind of contour map of the tachycardia. Physiologists now measure this map by detecting local activation events with computer-driven two-dimensional or three-dimensional arrays of extracellular pickup electrodes, or by raster-scanned optical interrogation of intracellular voltage-sensitive dyes: if done only on the outer surface of the ventricle it is called an *epicardial map*, or if only on the inner surface, an endocardial map. Since 1941 (Moe *et al.*, 1941) the contour lines of activation time on such a map have been called *isochron(e)s* (Fig. 1). I unknowingly re-coined this word (Winfree, 1967, without the "e" often used by cardiologists) in connection with the theory of spontaneously periodic dynamics. The concept is well developed mathematically in that context; its application in the context of this paper—to spatially extended systems the individual parts of which are not spontaneously periodic by themselves—must be regarded with caution.

The cardiac physiologist's isochron(e) representes a geographical locus of simultaneity: that is, along an isochron(e) the membrane activated simultaneously. The

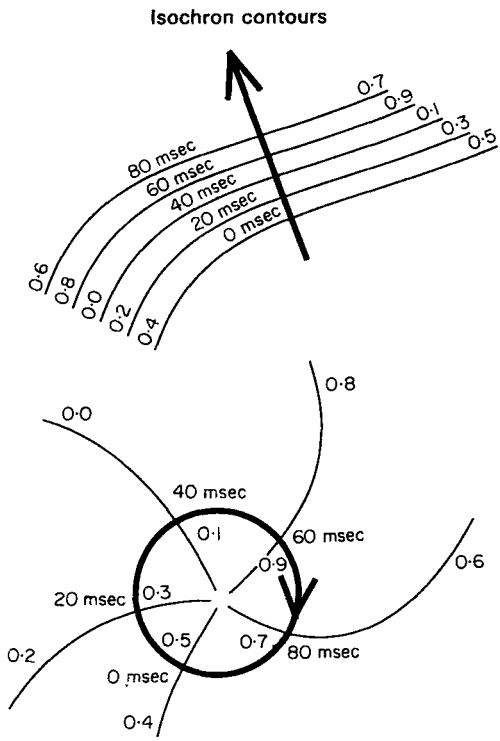

FIG. 1. Geographical contours along which a given event will occur or did occur simultaneously, or the corresponding loci in state space, are both referred to as "isochronal contours". Geographically, they can be more-or-less parallel as in familiar wavefronts (upper part of figure), being closer together where conduction is slower. They can also converge to a singular point in complete ordered sets spanning a full cycle (lower part of figure). In this case conduction speed dwindles to zero near the convergence. (More exotic things can also happen, e.g. in "meander": see below.) Labeled as isochrones, in msec, along the middle series of labels, each indicates the position of a wavefront at that time after a chosen time zero. Labeled as isochrons from 0 to 1 (identifying 1 with 0) along the inner and outer series, the label indicates the present state of fibers on that contour and moves with the contour: the series in which the 20 msec isochrone is at phase 0·2 labels states at time 20 msec. At time 30 msec, 10 msec later, the isochrons have all moved forward by 0·1: the 20 msec isochrone is then at phase 0·3. Although it is usual to calibrate "phase" in proportion to time, normalized to the temporal period of the cycle, it is not necessary to do so. In a situation such as this, where almost the same cycle of states may be repeated at quite different periods (lingering for a longer or shorter time near the rest state until re-excitation), the intent is to label the same state with the same number, regardless of period.

theorist's isochron represents states which precede or follow a certain event (e.g. activation) by the same interval of time, not necessarily 0. The geographical locus along which the membrane is all on the same state-space isochron is also called an isochron. In any *uniform* medium isochrons of simultaneous recovery fall exactly in the footprints of isochrons of simultaneous activation, though they generally do not in a medium with geographically graded intrinsic properties (Salama *et al.*, 1987). Isochrones and isochrons are similar, but their numerical book-keeping schemes differ as follows.

Physiologists label isochrones by the time (after some chosen zero, e.g. the moment of a stimulus) when that locus was at phase 0, i.e. was the wavefront. Isochrones are labeled by numbers increasing in the direction of propagation, and they do not move (see the upper panel of Fig. 1, with labels dimensioned in msec from an arbitrary time zero). In contrast, the theorist's "isochrons" tell something about the fiber's instantaneous state: its present and changing phase in the cycle of excitation and recovery (see the lower panel of Fig. 1, with labels dimensioned in tenths of a cycle). Isochrons are thus labeled by numbers increasing in the direction from which the wave propagated, and they move while retaining their physiological identity (see relabeling 10 msec = 0.1 cycle later in Fig. 1). The old isochrones deposited by a past wavefront are rigidly preserved and must be abruptly erased when a new wavefront intrudes. Isochrons in contrast continually change shape, rapidly where a wavefront is encouraging fibers just ahead to rapidly change their state, or, giving a simplified accounting of state, to rapidly advance their phase. Isochrones are readily determined by observations limited to bipolar extracellular electrodes, since one can thus know where a wavefront once was. Isochrons—depicting phase as a measure of the instantaneous state of fibers—can be determined using intracellular microelectrodes or voltage-sensitive membrane dyes. Isochrones may be thought of as historical positions of isochron 0, from which the changing positions of the other isochrons can be estimated if it is inconvenient to measure them directly. In this paper I use "isochronal contour" for both.

A phase singularity is a point where the isochronal contours of each phase in the cycle all come together in order, either geographically or in state space or (usually) both. Phase singularities become centers of vortex-like circulation of activity: they are the hinges on which re-entrant action potentials turn (Fig. 1, bottom). The convergence of isochronal contours near an ideally simple phase singularity (Fig. 1) implies slow conduction. This may or may not entail complete "*conduction block*". It may if the complete set of isochronal contours inside a re-entrant circuit do *not* smoothly converge, but terminate obliquely along a locus some cm's long where membrane potential changes in an apparently discontinuous way (Winfree, 1987, fig. 5.3; Dillon *et al.*, 1988; Shibata *et al.*, 1988; Allessie *et al.*, 1989). Isochronal maps are commonly sketched to include such "arcs of functional conduction block", but their reality in normal tissue (as opposed to ischemic tissue or thin-layer anisotropic preparations) remains conjectural so long as observations are limited by the low spatial resolution of presently available techniques.

Arrhythmia is a clinical term which might be better rendered as DYSrhythmia, because it just means abnormal departure from the familiar cardiac cycle, e.g. a tachycardia. It does not necessarily denote absence of rhythmicity, and in fact the more dangerous "arrhythmias" often start as strikingly regular rapid rhythms that only later degenerate into something really irregular. We will see that even at the earliest stage, the seed of utter irregularity is already there in isolated points called phase singularities, where activity *is* truly arrhythmic.

The critical phase, or "singular phase", of a cycle is a time when application of a certain kind of stimulus at appropriate strength results in arrhythmia in one or another sense, depending on context. Any phase of the cycle can be the critical phase, depending entirely on the nature of the stimulus. If the context is space-independent (an isopotential system such as a single spontaneously oscillating pacemaker cell) the "arrhythmia" consists of unpredictable (in the presence of "noise") timing of return to the former cycle, or failure to return. If the context is geographical (a spatially distributed oscillator or, as in this paper, a medium of excitable—but not spontaneously rhythmic—membrane driven by a pacemaker) then the "arrhythmia" may manifest itself in many geographically patterned forms which have in common only that they do not predictably revert to the prior rhythm. In geographical context the "critical phase" is not critical all by itself, but only as a representative middle value in a geographical gradient spanning a necessary range of phase around that representative critical phase.

A rotor is the neighborhood of the internal end (the "wavetip") of a wavefront in an excitable medium. This region usually does not propagate forward like the rest of the wavefront; rather, it turns in place while the attached wavefront wraps into an outgoing spiral around it. The wavetip (alias rotor) usually overlaps the pivot (alias phase singularity), but it need not: in media of marginal excitability, with parameters close to values at which propagation fails, the wavetip (rotor) can circulate around the pivot (phase singularity) at some distance (Pertsov *et al.*, 1984; Zykov, 1984; Jahnke *et al.*, 1989).

"*Vortex core*" or "re-entrant vortex" designates the neighborhood of the phase singularity, the pivot. The vortex is the wavetip and any larger region that it may circulate around. The vortex arises near the intersection of a contour of critical phase (in a phase gradient) with a contour of critical stimulus strength (in a stimulus gradient). All segments of the outgoing wavefront(s) can be traced backward to the nominal perimeter of the vortex, of length equal to one wavelength of the spiral wavefront radiating away. (A spiral's wavelength can be defined as the spacing of plane waves far from the source, or as the spacing of curved waves near the source taken along the local normal trajectory, which happens to be nearly a straight line tangent to the perimeter: Winfree, 1973, 1980.) Within the vortex core the action potential's waveform is conspicuously altered (e.g. it may have multiple ups and downs during a single period: Allessie *et al.*, 1976; Zykov, 1984; Jahnke *et al.*, 1988) and its amplitude is conspicuously attenuated (e.g. it may be essentially zero throughout a broad disk: Pertsov *et al.*, 1984.)

For the purposes of this paper "vortex" and "rotor" are practically co-extensive and I will not try to maintain the technical distinction between them.

3. Creating Phase Singularities by a Premature Stimulus

The viewpoint of this article is that if we want to understand management of re-entrant tachycardia in the mammalian ventricle, we should first understand the

creation (and perhaps the annihilation) of phase singularities. Creation corresponds to vulnerability to fibrillation; annihilation corresponds to cardioversion, and possibly to defibrillation. Defibrillation, to be successful, must avoid creation or recreation of phase singularities (Chen *et al.*, 1986*a*,*b*, in press).

To create a phase singularity one must deliver an appropriate stimulus at an appropriate time. This remark has three interconvertible interpretations:

(3.1) a local interpretation in terms of stimuli; and

(3.2) a local interpretation in terms of membrane mechanism; and

(3.3) a global interpretation in terms of stimuli.

Here we deal with the first and last topics briefly and the middle topic at great length.

(3.1) THE LOCAL INTERPRETATION IN TERMS OF STIMULI

The local interpretation in terms of stimuli provides a picture of the physiological geography in which a phase singularity is created. In the local interpretation we recognize that at each moment each part of the myocardium is at some local phase, T, in a cycle of repetitious activity. Each T is instantaneously realized along some moving geographical contour in the myocardium called an isochronal contour. One of these contours has the critical phase T^* for the kind of stimulus being used.

A stimulus electrode drives current through the myocardium to produce intense stimulation near the electrode and weaker stimulation farther away. This geographically graded stimulus thus creates contour lines of local stimulus strength, S. The intersection of a contour of critical strength S^* with a contour of critical phase T^* marks a neighborhood in which (given sufficient range of T and S around these central values) conditions can be perfect for starting reentry. Here there begins a vortex-like circulation of activity around a phaseless central point called a phase singularity. In normal excitable tissue the period of the rotor is, of course, longer than the refractory period, and may be much longer if, as in the numerical experiment presented below, reentry is limited mainly by failure of sharply curved wavefronts to propagate (Zykov, 1984).

Thus the onset of tachycardia can be analyzed geographically by attention to little more than the crossings of two critical contours: a contour of critical phase, T^*, and a contour of critical local stimulus strength, S^*.

The reasons for existence of "critical" contours, and for the apparition of a rotor and its associated phase singularity near their intersection, are the subject of section (3.2.3). But it should be noted here that the *neighborhood*, not the intersection itself, is crucial: if a cylinder around the intersection point is removed from an excitable medium, and the cylinder is much smaller than the rotor (its perimeter is much less than one wavelength) then its removal hardly affects the rotor (Pertsov *et al.*, 1984).

(3.2) THE LOCAL INTERPRETATION IN TERMS OF MEMBRANE MECHANISM

This section first (3.2.1) reviews a graphical technique for visualizing the changing geographical distribution of activity, when activity consists of two or more interacting local state variables. Then section (3.2.2) describes in those terms a geographical

arrangement of local membrane states that may be common to all varieties of reentry in two- and three-dimensional continuous media. Section (3.2.3) elaborates on section (3.1) above, motivating that "rule of thumb" for predicting the geographical locations and handedness of re-entrant vortices created by a vulnerable-period stimulus. Finally, section (3.2.4) leads into the "global" description (3.3) by laying out the conceptual basis for a myocardial pinwheel experiment.

3.2.1. *Geographical landmarks mapped into state space*

To envisage the geography of wave propagation in context of local membrane dynamics we begin with a snapshot of the instantaneous state of the entire medium. "State" means the location of each tiny homogeneous region of medium in an abstract state space whose dimensions quantify the electrophysiologically important variables of excitation and recovery. In the simplest possible (2-variable) caricature, those co-ordinates are the local membrane potential, V_m, and R, a local recovery variable representing aspects of refractoriness that are not nearly instantaneous functions of V_m.

During geographically synchronous activity all regions of the medium map to the same point in this state space. That point moves while the uniform medium traverses its excitation-recovery loop. Given any initial combination of V_m and R, the rates of spontaneous change of both V_m and R are completely determined. This rate of change can be represented geometrically by a tiny arrow at each point in the space. Collectively the field of arrows constitutes a continuous flow showing how the membrane spontaneously changes its state from any initial condition.

If we set aside baroque complications such as multiple co-existing limit cycles and/or rest states, multiple co-existing mechanisms of excitability, etc., then this flow has a common appearance in familiar cases (Fig. 2) despite the diversity of physical mechanisms underlying generic excitable media.

Figure 2(a) (right) resembles the FitzHugh–Nagumo membrane model (see Appendix), which is in turn a simplification of the Hodgkin–Huxley (1952) description of ionic currents in squid giant axon membrane. This includes only *some* of the currents known to exist in ventricular muscle membrane. A more elaborate model should represent ventricular electrodynamics more faithfully. For example, membrane potential would linger longer in depolarization (the "phase 2" plateau) then monotonically revert to resting potential while the recovery process also reverts to rest; this would remove the slight overshoot and "phase 4" depolarization seen in Fig. 2(a) (lower right), where potential rebounds from slight hyperpolarization while the recovery process is still vigorous. In this paper we retain the classical generic excitability model, not only to emphasize that the main features of re-entry derive from generic aspects of excitability rather than from idiosyncrasies of myocardium, but also because more advanced electrophysiological models have not been adequately tested in the context of two-dimensional reentry. (The first such tests have not encouraged replacement of more generic models: see the end of section 4).

If all points followed the same kinetics from the same initial disturbance off the resting state then the whole medium would be distributed in a strictly

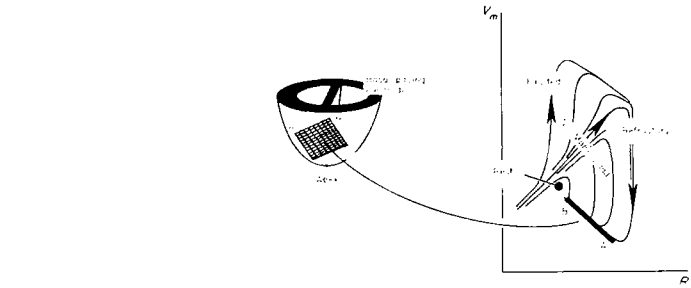

(a)

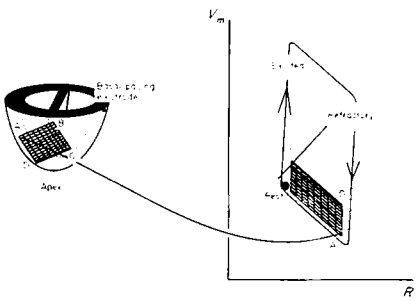

(b)

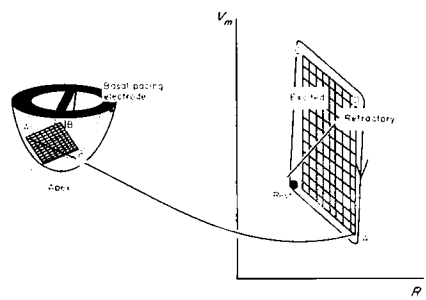

(c)

FIG. 2. (a) Each tiny region of myocardium, small enough to be considered electrically uniform, has some instantaneous V_m and R (and many more specific measures of ionic channel activity, but these two suffice for present purposes). On such a diagram each region can be mapped adjacent to its neighbors. An isolated region would spontaneously change V_m and R in a direction determined by its instantaneous values of both. In a typical excitable medium these vectors (sampled here as eight trajectories) approach a loop proceeding from states near "rest" through zones here labeled "excited" then "refractory", and back toward "rest". Trajectories in the interior "No-Man's-Land" generally diverge, some rapidly depolarizing upward and some rapidly repolarizing downward, from a separator trajectory that passes near the rest state and determines the strength-interval curve of classical physiology. During paced activation all regions follow the standard excitation loop from rest back to toward rest. Here a moment late in electrical systole is indicated, when points closer to the pacing electrode (e.g. side BC of an arbitrary coordinate grid ABCD embossed on the epicardium) have almost recovered from electrical activation and points further away (e.g. side DA) are not far behind. The tissue is thus organized by a timing gradient radial to the pacing electrode. In this gradient fibers with the same R also have the same V_m.

FIG. 2. (b) Tissue under the grid is again mapped into the (V_m, R) plane as in Fig. 2(a), but now fibers with the same R no longer also have the same V_m, due to application of graded (maximum at the apex) depolarizing stimulus transverse to the pre-existing timing gradient. On this and all subsequent (V_m, R) planes, the schematic trajectories are reduced to a mere cartoon: rest state, excitation-recovery loop, and portion of the separator that serves as a threshold (diagonal line).

FIG. 2. (c) As in Fig. 2(b), but the stimulus is strong enough to reach well beyond the separator. Here the initial gradient of R also spans the normal range, so all states inside the excitation loop are achieved and laid out in an orderly geographical pattern. Fibers far from the apical stimulus electrode are on the bottom of the grid in state space, scarcely displaced from their pre-stimulus states. Fibers imaged nearest the loop in state space are attracted toward it, and those suspended in No-Man's-Land become the rotor. The geographical locus of the separator becomes the wavefront, because it separates trajectories of rapid depolarization from trajectories turning more directly back down toward the rest state.

one-dimensional way along the common trajectory. But if the tissue's intrinsic properties are regionally variegated (refractoriness smoothly graded transversely (Salama *et al.*, 1987) or from endocardium toward quicker-recovering epicardium or if there were islands in which the refractory period lasts somewhat longer) then they would not all follow the same arrows. The image would then depart somewhat from the mean trajectory and might be complexly folded and stretched.

The co-ordinates V_m and R are of more use to electrophysiological theorists than to laboratory physiologists who can conveniently monitor only the local membrane potential (V_m, not R). In fact during cardiac dysrhythmias observed through bipolar extracellular electrodes, not even the local membrane potential is observed, but only the *time* when a traveling activation complex passed through the neighborhood of the electrode, and only then if its wavefront was not too nearly parallel to the bipole. Nonetheless, Fig. 2 provides an instructive framework for interpreting those times, and for interpreting the effects of a stimulus.

If the preparation is not space-clamped (and it never is in case of *in vivo* myocardium) then in any snapshot different regions typically map to different states. For example, if an activation wavefront has recently passed through the medium from a basal pacemaker site toward the apex, then regions remote from the pacemaker may be a hundred milliseconds behind regions adjacent to the pacemaker, while they all traverse a common path from the rest state through excitation and refractoriness back toward the same rest state. Figure 2(a) depicts a medium that is everywhere almost back to rest. The entire medium [sampled under a gridwork of electrodes Fig. 2(a)] maps to a short segment of trajectory on final approach to quiescence: depolarization has run its course everywhere (the whole image has come back down from high V_m) and the recovery process R is about to end. The entire two-dimensional or three-dimensional medium maps into state space as a one-dimensional image along an arc of the excitation-recovery loop.

A depolarizing stimulus, provided by current from an electrode at the cardiac apex for example, moves each affected region upward in state space by some membrane potential displacement. This is illustrated in Fig. 2(b). The gridwork is embossed on the epicardium to provide uniformly spaced landmarks; its image in state space would generally be quite distorted, but we have drawn a more orderly caricature in Fig. 2(b). If some regions (e.g. edge AB far from the apex) are affected less than others (e.g. edge CD near the apex) then the medium's image is stretched between its original location in state space (in tissue at edge AB far away from the apex) and a somewhat depolarized position (in tissue at edge CD near the apex). The previously-collapsed image of Fig. 2(a) is thus opened to cover a finite area of state space on the (V_m, R) plane.

If the stimulus near the electrode has sufficient strength to fully depolarize the membrane then the full range of possible depolarization is spanned. Given also an initial range of phases wide enough to span the excitation-recovery loop from left to right as in Fig. 2(b), the image of the affected region of the medium will cover enough of the interior of the loop [Fig. 2(c)] for local kinetics to pull it open like a rubber diaphragm spanning the loop.

If each region were now to independently follow its local spontaneous kinetics (the arrows) then they would all disperse outward to the loop and swirl along it

back toward the rest state. But they are not independent: they are coupled electrotonically through their intercellular gap junctions, so adjacent patches cannot diverge so far. If the medium has no hole then continuity is maintained across the interior of the loop in state space. The grid's image is stretched quite thin in the interior while most regions approach the bordering loop, but continuity is maintained. Most of the medium rides this loop, depolarizing and recovering normally as wavefronts sweep past. But regions suspended within the loop are stably trapped there by the topological character of the phase map.

3.2.2. *The common feature of all forms of two-dimensional reentry in uniformly excitable continua*

Continuity requires that some region must remain half-depolarized and half-refractory in states that FitzHugh (1961) called "No-Man's-Land" [Fig. 2(a)]. This tiny region of attenuated action potentials constitutes the rotor, which is or circulates around the eye of the vortex, containing the phase singularity. (In marginally excitable media the vortex need not be tiny: a vortex core bigger than the rotor may map to the rest state while the wavetip circulates around it without penetrating, Pertsov *et al.*, 1984.) Regions surrounding the vortex core move clockwise on Fig. 2 toward the rest state, near which they are pulled up into excitation due to their electrotonic connection to non-refractory neighbors just above threshold. So the cycling continues at a period longer than the refractory period by an amount that depends subtly on the two-dimensional geometry of propagation. Cycling can fail if:

(i) adjacent fibers cease to function almost identically, e.g. if the medium is pervaded by regions with quite different membrane properties (for example, near infarcts) or by non-conducting boundaries (for example, fibrous tissue in the aged), or if

(ii) the piece of medium monotonically spanning the excitation-recovery loop is physically so small that the boundaries of its image in state space can be pulled across No-Man's-Land. This "pulling" corresponds to the steepness of potential gradients, i.e. the magnitude of electrotonic currents. The currents flowing between membranes of unequal V_m tend to equalize those V_m's, pulling their images together in state space at a speed proportional to the potential difference and inversely proportional to their physical distance apart, i.e. proportional to the magnitude of potential gradient (Winfree, 1974*a*,*b*, 1978, 1980). The *boundaries* of a tissue (and of its image in state space) are pulled from just one side. Only the local kinetics [trajectories, Fig. 2(a), left] provide a countervailing contribution to the image's motion in state space, and this is not sufficient to hold the boundary on the excitation-recovery loop if the loop's full range of V_m is spanned in too small a physical distance. If the image of the medium folds several times over the excitation-recovery loop (i.e. several regions of incipient reentry are packed within its borders) then every region monotonically spanning the loop may be too small, and some or all of them will prove unstable. The pertinent scale of distance can be derived from the local electrophysiological parameters, and turns out to

be around 1 cm for myocardium. It has been appreciated for over a decade that reentrant circuits in myocardium can be this small (Wit & Cranefield, 1978). Numerical experiments and laboratory experiments summarized below provide further quantification.

If the vortex region of tissue trapped inside the excitation-recovery loop is not too small, and not lacerated by discontinuities, then its image is not stretched too tightly over the excitation-recovery loop and remains smoothly connected. Any mapping of tissue geography into the state space (any geographical distribution of local states) which thus substantially overlaps the interior of the excitation-recovery loop [e.g. Fig. 2(c)] then provides a *sine qua non* for reentry in the fully two-dimensional, vortex-like mode. This simple geometrical criterion suffices for reliable design of numerical experiments involving intricate two-dimensional and three-dimensional re-entry, and for design of practical laboratory experiments in chemically excitable media and in cardiac muscle. It should be made more precise, but after a decade of wrestling with it, I still cannot do better.

Moe *et al.* (1964, p. 210) derived a seemingly different *sine qua non*—inhomogeneity—for re-entry in *dis*continuous media. Since myocardium is for some purposes electrically continuous but for other purposes (or in diseased states) is almost discontinuous, one may wonder whether either "*sine qua non*" can be a necessary and sufficient criterion. My belief is that they both are, if the inhomogeneity required by Moe and co-workers for induction of reentry be sometimes interpreted as the fleeting orderly inhomogeneity of membrane state here described. In other words, it need not be (Winfree, 1989*b*) the small-scale disorderly intrinsic inhomogeneity of membrane properties originally described, nor even the orderly gradients of intrinsic membrane properties over larger spatial scales described more recently (Allessie *et al.*, 1976; Boineau *et al.*, 1980; Gough *et al.*, 1985).

To create one or more phase singularities in an unbounded continuous excitable medium with geographically uniform coupling and membrane properties, it is only necessary to hang the medium's image over the excitation-recovery loop. There are diverse ways to induce such a mapping from the geographically-distributed medium to its state space. I think they correspond to the diverse ways to evoke reentry. Unless the inducing stimulus strongly affects the entire medium, the singularities (and surrounding vortices) necessarily arise in mirror-image pairs (Winfree & Strogatz, 1983). Rotor pairs (now called "figure-eight" reentry) do commonly appear on epicardial maps after a premature stimulus (Allessie *et al.*, 1976; El-Sherif *et al.*, 1981; Wit *et al.*, 1982; Mehra *et al.*, 1983, El-Sherif, 1985, 1988, Downar *et al.*, 1988). Figure 3 shows an example in the human left ventricle. In some instances this pairing is attributed not to the mechanism here proposed, but to large-scale permanent heterogeneity in the medium, e.g. an island of temporarily lingering refractoriness that cuts a gap of conduction block out of a passing wavefront (see section 4 below). But permanent anomalies are not necessary: paired rotors are a generic consequence of local stimulation in excitable media. For examples without necessary involvement of anisotropy, using the "method of successive adjacent stimuli", see Winfree (1985). In bidomain anisotropic media paired rotors may generically occur even following successive stimuli at one electrode, as in electrophysiological testing via cardiac

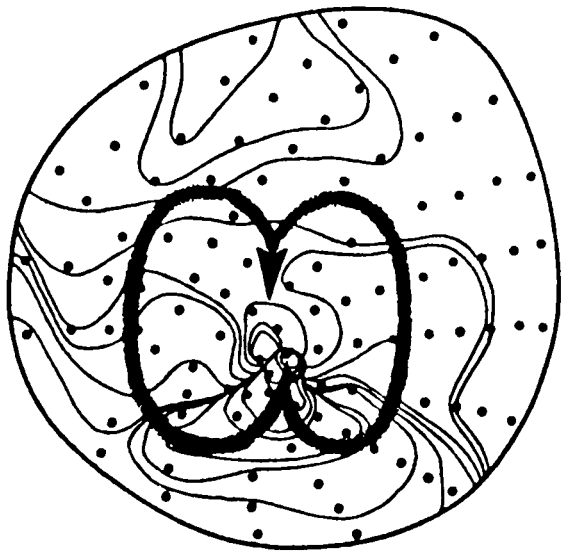

FIG. 3. "Figure-eight ventricular tachycardia" clinically induced by three premature stimuli and exposed by endocardial mapping in the human left ventricle. Isochronal contours are 12 msec apart; their time sequence is indicated by the superposed thick line with arrowhead. In this polar projection the apex is near the midpoint of the twin vortex and the septum is on the left. The dots are electrode sites. (Adapted from fig. 3 of Downar *et al.*, 1988.)

catheter electrodes (Winfree, 1989*a*). Pairing is the rule in perfectly uniform (chemical) excitable media far from boundaries (Winfree & Strogatz, 1983; Winfree, 1987).

In a bounded medium, a rotor too close to a non-conducting barrier can vanish into it, leaving only the one of a created pair that was more remote from the boundary. In terms of Fig. 2, this vanishing act consists of the image of the medium's boundary being pulled across the middle of the excitation-recovery loop, due to its one-sided attachment to medium inside the loop (in geographical terms, in the rotor, the wavetip). The wavetip or rotor, in other words, swiftly falls into the boundary. This may be the origin of the single rotors that are seen in confined media about as commonly as mirror-image pairs, e.g. Fig. 4. Such pairs, if too close together, also commonly mutually annihilate and vanish by a similar mechanism in diverse calculations using a variety of excitable media (Winfree, Reiner, Nandapurkar unpublished results). The state-space image of a piece of medium containing adjacent mirror-image rotors is folded double, each part of both rotors occupying the same state. Each half precisely resembles a single rotor adjacent to a boundary. Unlike any other place, the fold line is pulled with double vigor from one side of the rotating image in state space, and passes over the interior in an act of mutual annihilation.

3.2.3. *Rotors arise near intersections of critical contours*

The regions imaged inside the excitation-recovery loop (in No-Man's-Land) are those realizing combinations of V_m and R simultaneously intermediate between the

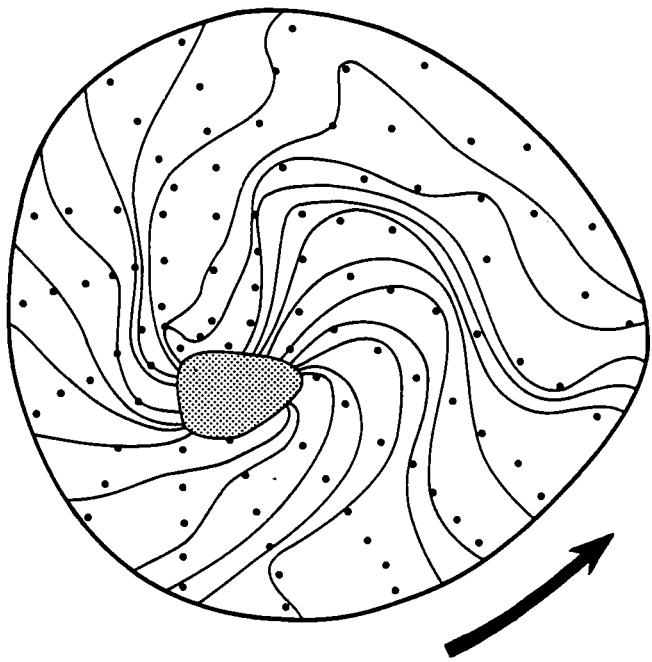

FIG. 4. Ventricular tachycardia (a single anticlockwise vortex) on the human ventricle, exposed by epicardial mapping. Isochronal contours are 12 msec apart. In this polar projection the apex is near the center and the atrio-ventricular ring is the perimeter. The dots are electrode sites. Electrode spacing is too coarse in the areas stippled gray to resolve the many contours converging there. (Adapted from fig. 8 of Downar *et al.*, 1984; fig. 5.4 of Winfree, 1987).

extremes realized in a normal action potential. Diverse numerical experiments indicate that these are usually regions quite close to those which realize such combinations in the first moments following the critical stimulus. The rotor thus arises near regions stimulated at times near T^* with intensities widely straddling S^*, these special values being those which achieve a mid-loop combination of V_m and R. In the case of a depolarizing stimulus, T^* occurs along the excitation-recovery loop when R is about midway between its extremes (at the lower of the two such phases), at which time the required S^* perturbs V_m to lie between the membrane potentials characterizing those two phases (Fig. 5).

In geographical terms, regions that are at phase T^* when the stimulus strikes constitute an isochronal contour some distance behind the activation front. Regions stimulated at critical strength constitute a closed ring some distance from the stimulus source, e.g. an intracellular depolarizing electrode. Where these critical contours cross (generally twice, in mirror-image fashion, if one of them is a closed ring), both conditions are met: that neighborhood is in No-Man's-Land and is surrounded in an orderly way by regions much closer to the normal excitation-recovery loop, all the successive states along it being arranged in order around the perimeter of the central regions. That center becomes a rotor, the source of a reentrant vortex.

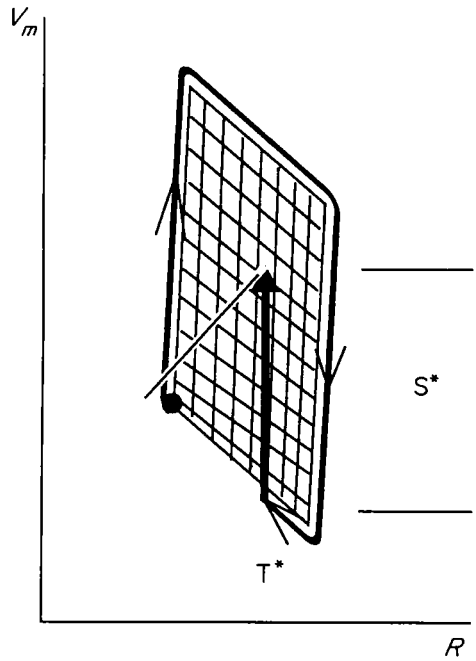

FIG. 5. The right side of Fig. 2(c) is relabeled to show a "critical" stimulus strength S^* needed to reach interior No-Man's-Land from a "critical" phase T^* during normal excitation and recovery. These values are critical only in the sense that they characterize the "No-Man's Land" zone in state space that must be spanned in order to cover the excitation-recovery loop; if they are not conjointly realized then the necessary conditions for reentry are not attained.

To put the same principles more generally for other agencies of stimulation than direct depolarization, T^* occurs along the normal excitation-recovery loop on the "upwind" side of the loop's center (the side from which the stimulus pushes the state into No-Man's-Land, Fig. 5). And S^* is the stimulus strength required to move from there to mid-cycle in whatever direction characterizes that stimulus modality. (The direction would be oblique if some combination of neurotransmitters and electric current could be used as stimulus.)

In the case of a depolarizing stimulus (the net effect some milliseconds after current passes in any direction between *extra*cellular electrodes), T^* occurs during a late stage of repolarization. This happens to be near the time of the electrocardiogram's "T-wave" when some regions have repolarized and, other regions, because they were depolarized in sequence spanning almost 100 msec while the activation front propagated through the medium, have not yet repolarized. That orderly repolarization creates the electrocardiogram's T-wave. It is also believed that even simultaneously triggered adjacent fibers may make their way around the excitation-recovery loop at significantly different rates, repolarize separately, and regain excitability separately. If so then this interval may also be characterized by enhanced local non-uniformity of membrane state *en route* to uniform rest. This

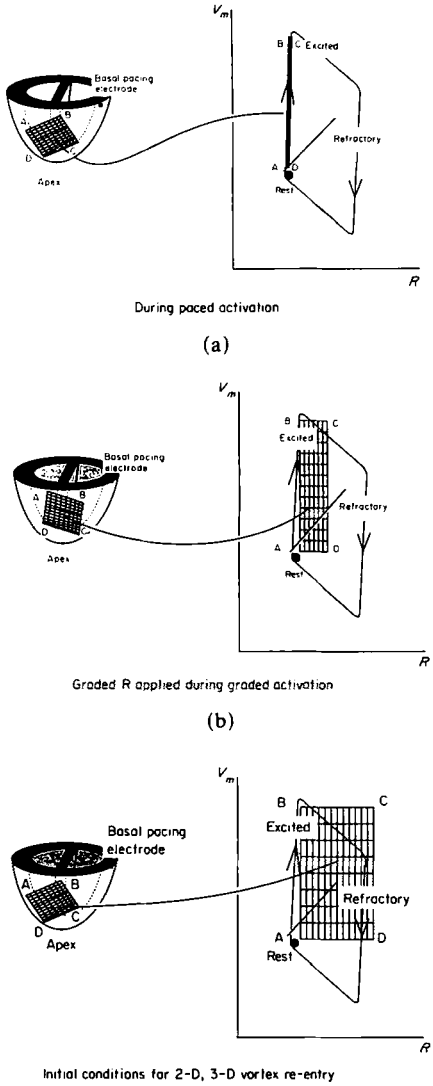

FIG. 6. (a,b,c) As in Fig. 2 (a,b,c) but the stimulus pushes the membrane state to the right instead of upward (e.g. opens the potassium channels neurochemically instead of opening sodium channels electrically).

idea figures prominently in conventional interpretations of vulnerability, but it is *not* the reason for vulnerability to reentry in Figs 2 and 5.

A thought experiment dramatizes the distinction between the classical interpretation of T^* (vulnerability during the T-wave) and the interpretation advanced here. Suppose it were possible to apply a neurotransmitter stimulus to quickly move R to the right as in Fig. 6 instead of moving membrane potential up as in Fig. 2. Then

T^* would occur not during recovery, at the moment of maximum dispersion of refractoriness, but during initial activation (Fig. 7). Once again, this is on the "upwind" side of the loop's center. The range of R to be spanned is roughly the normal range spanned by the excitation-recovery loop, as also in the case of depolarizing stimuli in Figs 2 and 5. The range of V_m necessary to span the loop is provided not by local heterogeneity, but by prior passage of the activation front at finite speed through the region to be stimulated, also as in the case of Figs 2 and 5. (Of course in damaged tissue it might be provided as much or more by local heterogeneity.) The essential idea here is that the mechanism of vulnerability in undamaged tissue as addressed in this paper and in Winfree (1980, 1982, 1983, 1987) is independent of "non-uniform dispersion of refractoriness" as usually conceived. The relative importances of the two mechanisms could in principle be assayed by an experiment such as suggested in Figs 6 and 7. Or if a geographically *uniform* stimulus could be shown to induce reentry, the mechanisms emphasized in this paper would be excluded: they crucially involve orderly gradients of local stimulus strength.

In any case the upshot is that, far enough from boundaries and given widely ranging V_m and R, it is not necessary to carry around all the theoretical baggage of Figs 2, 5, 6 and 7. To study the onset or the elimination of ventricular tachycardia (which may degrade into fibrillation, depending on the geographical complexity of the vortices) it should suffice to study the geography of critical loci, specifically of their intersections.

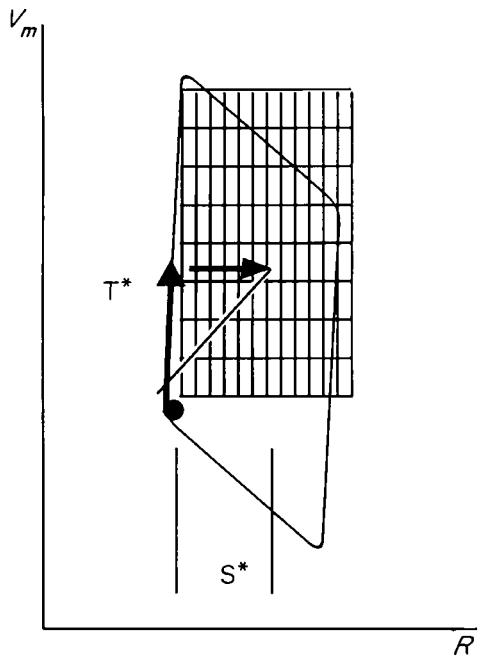

FIG. 7. As in Fig. 5 but corresponding to Fig. 6(c) rather than to Fig. 2(c): T^* occurs during the sodium inrush.

To summarize, then: there is a critical local phase T^* and critical local stimulus strength S^* that places the local state in the middle of the excitation-recovery loop in state space. In so doing it arranges neighboring places into state space and neighboring states into real space so that (if the ranges of T and of S are sufficient and the medium is large enough) a rotary aftermath is favored. If intercellular conductivity is sufficiently high to ensure that neighboring places stay similar in their membrane potentials, then this condition persists: reentry, leading to tachycardia, often leading to fibrillation, can start with phase singularities. The practical question is whether or not it commonly does. Phase singularities are not usually present in heart muscle, but they can be created in a generic way by a stimulus impinging on any medium whose local dynamics somehow contains a cycle, e.g. any oscillator or clock or just an excitable medium that does not cycle spontaneously so long as its state returns to rest along a standard cycle. Our objective here is to understand this fact well enough in the context of ventricular myocardium to design an experiment. In this experiment reentry will be elicited at a predictable location by a single stimulus of correctly chosen size and timing.

No mathematical theorems have been discovered which bear on this discussion of the creation and annihilation of rotors in non-oscillating excitable media described by reaction-diffusion equations (although there is plenty of mathematical analysis in print: see Zykov, 1984, and the supplementary references in the preface to that book). These qualitative and graphical arguments merely summarize 15 years' experience in watching such images on computer terminals during the computation of re-entry in continuous isotropic or uniformly anisotropic media, using diverse specific kinetics. The intended application to cardiac muscle does not follow rigorously, but only by metaphor. To pursue this application, section 3.2.4 simplifies the geometry and electrophysiology of mammalian ventricular myocardium to retain only what I regard as the essentials. We will return to numerical experiments in section 4, using one simple model of neuroelectric excitability.

3.2.4. *The 2-dimensional pinwheel experiment*

Figure 8(a) left is a sketch of the mammalian ventricles, showing the left and right ventricular chambers and the thick muscular wall that contracts around them, bounded by the atrioventricular ring. To keep the picture simple, consider the ventricles as though made of modeling clay and distort them into a disk, like a polar projection seen from below, with the endocardial surfaces exposed on top [Fig. 8(a), right]. These surfaces are covered with Purkinje fibers which convey into the muscle the action potential coming from the sinoatrial pacemaker node [Fig. 8(b)].

About once a second (in resting man) an action potential strikes this surface (not entirely synchronously) and sweeps through the 10 mm thickness of the muscle at about 0.5 mm/msec, emerging through the epicardial surface. Complete transmural activation takes about 60–70 msec. There is no further activity until the next impulse arrives about 1000 msec later.

These events can be observed in much finer detail now with arrays of epicardial electrodes spaced only 2–3 mm apart (Ideker *et al.*, 1987, Witkowski & Penkoske,

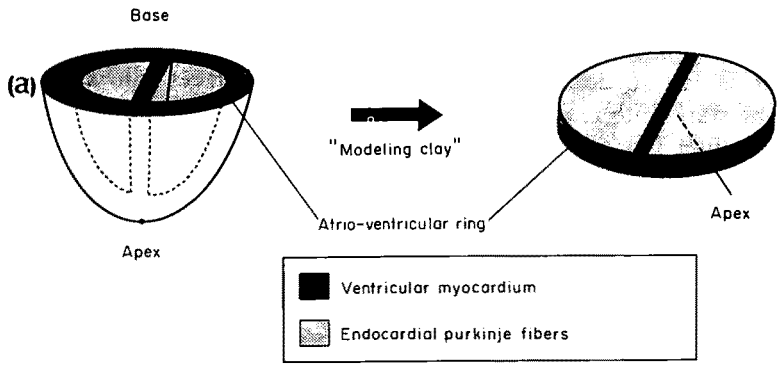

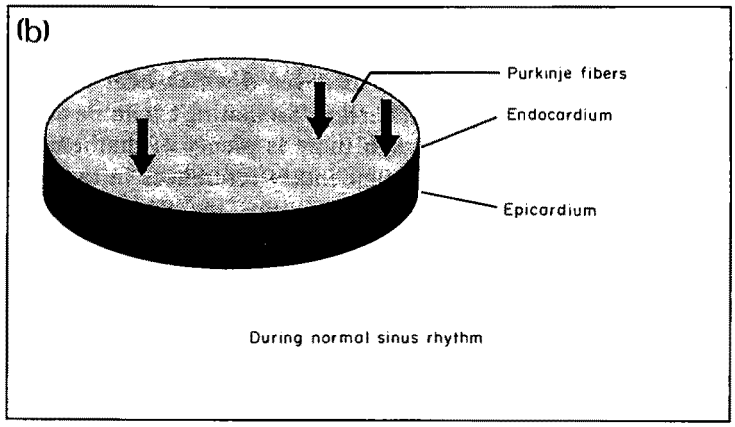

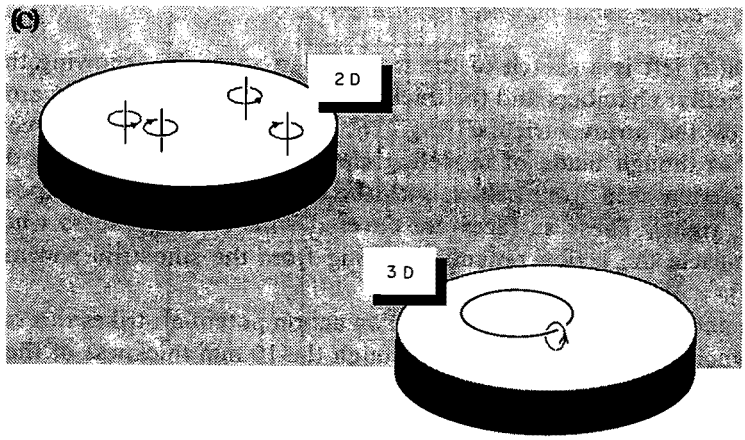

During Re-entrant tachycardia

1988*a*,*b*.) The electrotonic space constant of this medium is on the order of 1 mm during rest (varying of course during excitation and repolarization, and during ischemia) so this electrode spacing is almost as fine as needed to resolve the pertinent details. During normal sinus rhythm the isochronal contours are roughly parallel curves, much as on a contour map of a landscape (Fig. 1, top). But measurements during reentry show the fundamentally different contour topology of Fig. 1, bottom: excitation is always present somewhere, circulating around arrhythmic pivots. In three dimensions these pivots resemble vortex lines, usually created in mirror-image pairs (Chen *et al.*, 1988; Frazier *et al.*, in press) [Fig. 8(c), left].

We proceed now by considering the format of an idealized experiment contrived to induce phase singularities in an excitable medium at crossings of critical contours, thus putting these ideas to a crucial test. This is called the *pinwheel experiment* because it was designed to nucleate a pinwheel-like circulating wave. The pinwheel experiment was first done in 1967 in an entirely different context: the control of timing in circadian clocks (Winfree, 1986*a*). Successive experiments in different chemical, biochemical, and physiological systems are reviewed in Winfree (1980, 1986*a*, 1987). By applying the ideas behind the pinwheel experiment to a wider and wider range of cases, we are ultimately led to guess what must happen in healthy rhythmic heart muscle if the dominant factors are roughly those emphasized above. What must happen is tachycardia, perhaps leading to fibrillation.

Here is the general layout of the pinwheel experiment in cardiac context. For the sake of simplicity we return to two dimensions and imagine an activation front sweeping through the tissue as indicated in Fig. 9(a). For present purposes we suppose activation is synchronous from endocardium to epicardium, but propagates laterally, as can be artificially arranged by blocking the sinus impulse that would otherwise arrive at the endocardial surface through Purkinje fibers from the AV node, and instead pacing electrically from the edge of the ventricle rather than from its inside. Figure 9(a) is an epicardial view from the underside of Fig. 8(b) or (c) (a polar projection of the southern hemisphere of the heart as in Figs 3 and 4) with a pacing electrode at the top of Fig. 9(a) on the atrioventricular ring. The isochronal contour corresponding to the activation front ($T=0$) is indicated, along with the isochronal contour where membranes are momentarily at their critical phase, T^* (during recovery behind the front, if we anticipate giving a depolarizing stimulus.)

In the global interpretation (section 3.3), the vulnerable period is the range of coupling interval during which this critical contour is present somewhere within the

FIG. 8. (a) The ventricle is deformed into a thick disk for convenience of diagrammatic presentation in the next few figures. Its bounding surfaces are the atrio-ventricular ring and top edge of septum (and the endocardium and epicardium). (b) During normal sinus rhythm the ventricles are activated from inside (endocardium) by stimuli conveyed at intervals along the Purkinje fibers that cover the endocardial surfaces. Excitation then passes through the thickness of the muscle from inside (endocardium, top of disk) to outside (epicardium, bottom of disk). In the experiments to be described the disk is instead activated from a point on its rim (on the base of the ventricles, near the atrio-ventricular ring, as in Fig. 2). (c) During re-entrant tachycardia the disk is activated by vortices, often paired. They appear 2-dimensional in any plane parallel to epicardium (upper left) but are actually 3-dimensional and need not be upright as in the upper left diagram: given more a generic stimulus, the vortex filament might be an intramural vortex ring (see Winfree, 1989*a*).

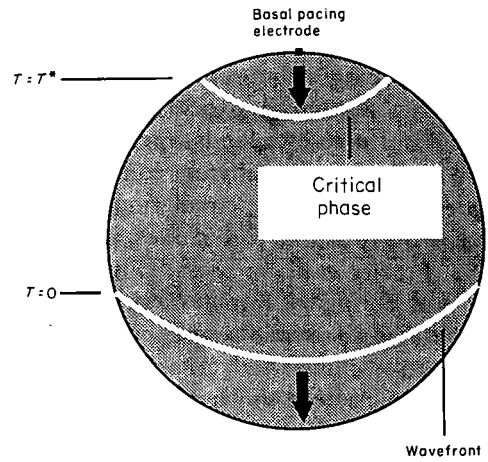

(a)

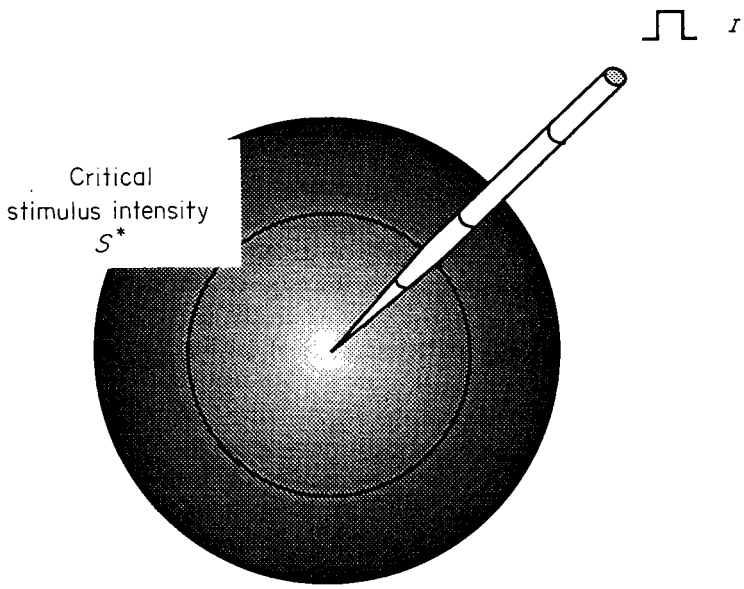

(b)

FIG. 9. (a) The disk of Fig. 8(b) is seen from the bottom (epicardial) side. Isochronal contours for a paced beat are indicated at $T = 0$ (wavefront) and at the critical phase T^* (in the wake of the wavefront). Note that the physiologist's convention would label each past position of the wavefront as an isochrone, by the time (referred to any chosen zero, e.g. the moment of an instigating stimulus) when the wavefront reached that position. This paper labels them in the opposite order, by "coupling interval": the time (referred to the moment of the reentry-inducing stimulus) since the wavefront activated that locus. (b) An extracellular electrode provides a pulse of current I to create a radially-graded depolarization, strongest near center. The critical range is centered along the black circle. A circle indicating diastolic threshold would be much further out [see Fig. 10(b)].

myocardium, or more specifically, anywhere within range of a certain stimulus, which we now turn to consider.

Figure 9(b) represents a stimulus of spatially-graded strength, e.g. an electric current delivered through an electrode at the apex. If the heart were a huge sheet of cellular membrane then intracellular injection here would depolarize or hyperpolarize in a straightforward way. Actually the membrane is convoluted into bundles of cylinders, and current can be administered only extracellularly to the bulk medium. The effective stimulus in the latter context is the local current density (Frazier *et al.*, 1988*a*). In an idealized geography it is constant along any ring around the electrode and the total current density falls off from ring to ring with increasing distance from center. The rings are drawn as circles; more realistically they would be ellipses due to anisotropic conductivity (Plonsey & Barr, 1984; Chen *et al.*, 1986a). A ring of critical stimulus strength $S = S^*$ is indicated.

Figure 10(a) emphasizes the neighborhood of an intersection of the two critical contours, $T = T^*$ and $S = S^*$: near here we expect reentry, creating a phase singularity. Every region mapped above the separator (see Fig. 2, captions) immediately begins to depolarize; regions below, if they depolarize at all, do so only later and only because of their connection to regions already depolarizing. The separator thus maps near the boundary of the immediately depolarized region close to the electrode, mostly behind the T^* isochronal contour [Fig. 10(b)]. Where it comes close to the rest state in Fig. 2, the separator trajectory acts like a threshold sharply separating two behaviors, adjacent trajectories diverging upward or downward. But this "threshold" becomes less sharp further inside the excitation-recovery loop where trajectories all begin to point down (repolarizing); regions mapped beyond this end (at greater R) contain no wavefront, so the wavefront has ended. Moreover, to the right of mid-cycle, the upward flow in the smaller range of V_m above the separator is slower than the downward flow in the larger range of V_m below the separator; this generally precludes forward propagation in excitability models or even induces propagation (of a repolarizing front) in the opposite direction (Tyson & Fife, 1980; Tyson & Manoranjan, 1984; Tyson & Keener, 1988), creating a wave *back* (see description of Fig. 12). The wavefront, ending in state space in No-Man's-Land, then pivots in the medium as shown in Fig. 10(b). It is convenient to choose the T and S contours intersecting in the medium near this region as the T^* and S^* critical contours.

In another experiment, if no intersection occurs between these critical contours, then no reentry results. But if intersection occurs somewhere then it is easy to imagine it happening twice, in symmetric mirror-image neighborhoods as in Fig. 10. Where do these pairs arise? That depends on the timing and size of the gross stimulus applied to the whole medium:

Given the diameter of critical-strength ring there is a range of coupling intervals—which I identify with the vulnerable period for that stimulus—when the critical phase contour can cut the critical stimulus ring [Fig. 11(a)]. The new wavefront follows the geographical image of the separator. From its pivot near the intersection of critical contours (which are defined so as to ensure that much) it extends in the direction of decreasing S and increasing T (because the separator is reached by slighter depolarization from later phases along the excitation-recovery loop). At

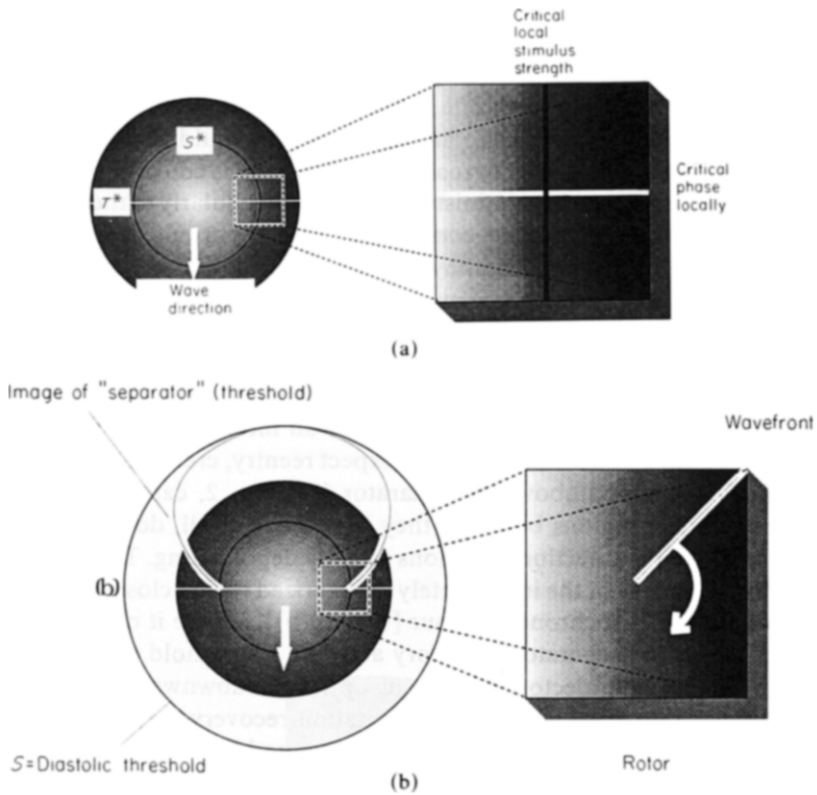

FIG. 10. (a) As in Fig. 9(b) but with the T^* locus superimposed in white, and with a square near one of the two intersections of T^* and S^* contours magnified for use in later figures. The T^* locus is moving behind the prior activation wavefront as indicated. (b) As in Fig. 10(a) but in the right panel the T^* and S^* contours are removed after the stimulus is delivered, and in both panels the geographical locus of the separator is superimposed, up to a level of refractoriness at which the wavefront that it defines no longer propagates forward. The portion shown is the propagating portion of the boundary of the region stimulated beyond local threshold. It extends from threshold displacement above the rest state (on the S = diastolic threshold contour) to fade away near the intersection of T^* and S^* contours. See Fig. 12 for its realization using a numerical membrane model.

each of the several possibilities for intersection illustrated in Fig. 11(a) the wavefront is drawn with that same decrement of S (radially) per increment of T (horizontally) from T^*, S^* (which placed the medium in the same state in each case).

Depending on the nature of the stimulus, it might move the local state in a different direction on the (V_m, R) plane (e.g. electric current hyperpolarizing the membrane as in Fig. 10 of Winfree, 1985, or a neurotransmitter altering some ionic channel that directly governs R as in Fig. 22 of Winfree, 1978). The values of S^* and of T^* depend on this direction. As emphasized in Figs 6 and 7, T^* generally does *not* coincide with the moment of maximum dispersion of refractoriness, though it happens to come close in the case of depolarizing excitation. In other cases the sense of rotation may be opposite and the wavefront's direction out of the intersection is different by an angle in the medium related to the rotation of stimulus direction

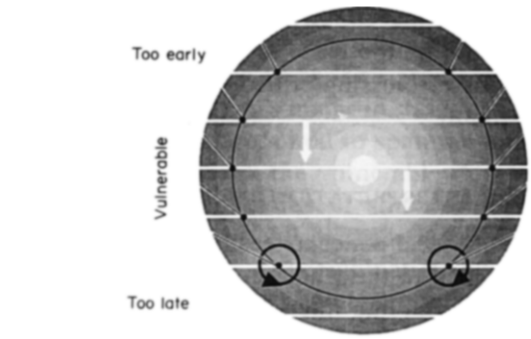

Coupling intervals for creation of mirror twin rotors

(a)

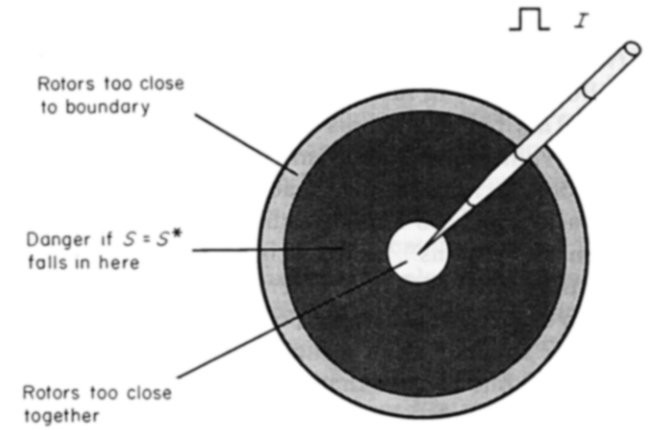

Upper, lower limits of vulnerability for creation of mirror twin rotors

(b)

FIG. 11. (a) As in the left-hand parts of Fig. 10 but the T^* contour is shown (horizontal white lines) in several consecutive positions ranging from "too early" to cut the S^* contour, to "too late". In five of the seven positions shown, T^* and S^* intersect. In each such case the pivoting wavefront is sketched (paired diagonal lines) roughly where it would arise if the stimulus had been given just then. This range of times thus accounts for vulnerability to reentry at this stimulus size, I. (b) As in Fig. 9(b) but instead of one S^* ring a continuum of them are indicated by the dark annulus, ranging from those too small to create independent rotors even when intersected across the diameter, to those too large to create rotors free of the medium's boundary. This principle establishes the existence of upper and lower stimulus-size limits of vulnerability to reentry (whence, perhaps, to fibrillation). Quantitatively, limits depend sensitively on electrode shape and the shape of the activation wavefront relative to the shape of the medium.

in state space. (For more on this "phase problem" see Winfree, 1989*a*, and the Appendix.)

Given a position for the moving contour of critical phase, it will encounter the ring of critical stimulus strength only for a limited range of voltages applied to the electrode. To refine this basic principle, remember that the critical contours only mark the midlines of necessary *ranges* of graded phase and strength. To span the needed range of initial conditions rotors cannot be too close together: the ring

should be large enough to ensure that the two crossings are not too close together, yet not so large that both would lie too close to (or beyond) the tissue boundary. This local description in terms of crossing critical contours leads us to the global interpretation in terms of stimuli.

(3.3) THE GLOBAL INTERPRETATION IN TERMS OF STIMULI

The T and S used above are *local* concepts easily confused with the timing and size of the gross stimulus applied to the whole heart. To distinguish them, we call these *global* variables CI, for "coupling interval" rather than "phase", and I, for total "current" rather than "strength". The "vulnerable period" at any given I is interpreted as the range of CI for that I, and "vulnerable domain" refers to the range of (CI, I) combinations, during which T^* and S^* contours can intersect somewhere within the medium. The possibility of confusion stems from the obvious similarity of the two stimulus coordinate schemes. Chen *et al.* (1986*a*,*b*, in press) and Winfree & Guilford (1988) in fact (mis)use the term "vulnerable period" in a local sense, like T^*. This paper attempts to keep the local stimulus description (T, S) and the global "vulnerability diagram" (CI, I) conceptually quarantined.

We move among altogether four distinct "spaces" in this paper, creating additional opportunity for confusion. I try to minimize this by referring to areas in the real, geographical medium as "regions", to areas in the local (V_m, R) state space as "zones", to areas in the global (CI, I) "vulnerability diagram" as "domains". (It is not necessary here to discuss areas in the (T, S) local stimulus plane.) The measure of the local stimulus is "strength" and of the global stimulus, "current".

Referring to Fig. 11(a), one can see that with a smaller stimulus, I, the contour of critical local stimulus strength S^* is smaller, so that the interval during which the T^* contour passes across a region surrounding the electrode (thus making the medium vulnerable if the stimulus were then delivered) is proportionally smaller [Fig. 11(b)]. If too small then the two mirror-image rotors would have been just a little closer together, and would have promptly annihilated one another. This occurs in the extreme case of I so small that the S^* ring vanishes because S then barely reaches S^* and does not map part of the medium's image all the way to the top of the excitation-recovery loop. In less extreme cases nascent rotors begin to form but overlap so substantially that neither fully develops, and excitation dies out after one or a few abortive rotations. This minimum distance for avoiding mutual annihilation between mirror-image rotors is roughly $1/\pi$ times the wavelength of the spiral, i.e. the conduction speed times the period/π.

With a larger stimulus, I, the two intersections are farther apart, so the two rotors and their nearby phase singularities are farther apart and out of each other's way. They persist, filling the medium with short-period waves. But if the stimulus were so strong that the contour of critical local stimulus strength lay too near the medium's boundaries, then once again the rotors would be unstable and there would be no lasting consequence. Or if it were so strong that the entire medium is stimulated beyond S^*, there would be no intersections. Thus there is an *upper limit to vulnerability.*

If the stimulus arrives almost too early or too late for the $T = T^*$ isochron to intersect the $S = S^*$ circle for the given stimulus current, I, then we have nearly-merging nearly-tangential intersections. The gradients of T and of S are almost parallel in this case, so the medium's image in state space is nearly one-dimensional, rather than two-dimensional as required to span the excitation-recovery loop.

These four extreme cases flank the vulnerable domain on four sides. Between these cases lie extreme combinations of stimulus CI and I which completely surround the vulnerable domain. All of them fail to spread the medium's image over the excitation-recovery loop, for combinations of the reasons given above. We thus expect a thin domain of (CI, I) combinations fringing the vulnerable domain on all sides, that elicit only a brief run of tachycardia as the two complementary nascent rotors annihilate one another or encounter the medium's boundary. (Figure 6.3(a) of Winfree, 1987, is misdrawn in this respect: the fringe was omitted on top.)

The domain of (CI, I) combinations that admit creation of paired vortices is molded delicately by electrode shape, tissue anisotropy, activation wavefront shape, and tissue boundary shape. (These subtleties leave much room for optimization of electrodes to defibrillate without at the same time creating phase singularities, i.e. without restarting reentrant tachycardias that might promptly reinitiate fibrillation.) This "black hole" (Winfree, 1987, pp 141–144) is a domain in the global interpretation's (CI, I) vulnerability diagram, not in the state space featured in the local interpretation—which may or may not incidentally contain its own "black hole" zones, reachable by stimulus combinations that place the medium within the attractor basin of a rest state. (My use of "black hole" for both has induced confusions, so I recommend dropping the metaphor altogether henceforth.)

This is about as far as I care to go with qualitative inference from simplified diagrams. The same endpoint was reached in Winfree (1983, 1987) by simplifying the description of excitable media involving two or more variables (Winfree, 1974*a*,*b*, 1978, 1980) to the didactically more convenient single-variable language of "phase" and "phase singularities". This device resembles the simplification to a single variable (membrane potential rather than phase on an excitation-recovery loop) intuitively employed by electrophysiologists; but everyone knows that such convenience is paid for by loss of reliability. Can the endpoint reached above also be reached by going in the other direction, not toward conceptual simplification, but toward numerical complexity? Can we implement a specific electrophysiological model in the digital computer to more quantitatively design a pinwheel experiment that could be executed in mammalian ventricular myocardium?

In short, the answer is "yes", and Figs 12 and 14 show the main results (see Appendix for more detail).

4. A Numerical Design for the 2-dimensional Pinwheel Experiment in Myocardium

This experiment was planned in the early 1980's (Winfree, unpublished seminars) using McKean's piecewise-linear two-variable caricature of an excitable medium (McKean, 1970; Winfree, 1974*b*), which is a simplification of the FitzHugh-Nagumo simplification (FitzHugh, 1960, 1961) of the electrophysiological description of squid

axon membrane by Hodgkin & Huxley (1952). If a more reliable quantitative electrophysiological model of ventricular myocardium were available, it would have been used; the Beeler-Reuter model (1977) did not seem better in respects that are vital to this effort. For this paper the design was reworked using the FitzHugh-Nagumo membrane model.

Figure 12 depicts the development of reentry after the vulnerable-phase stimulus. Six post-stimulus panels (c-h) are preceded by two panels (a, b) indicating the critical stimulus conditions. All panels show a 75 mm × 150 mm rectangle (about the size of the canine ventricle used in the corresponding experiments of Shibata *et al.*, 1988) represented by 11 250 "fibers". Each is programmed to follow FitzHugh-Nagumo membrane kinetics and to exchange current with its neighbors according to the cable equation (see Appendix) as though the whole myocardium were a single huge sheet of membrane. There is no calcium process to prolong refractoriness beyond the 40–70 msec (depending on stimulus size) of these sodium/potassium action potentials to values observed in canine myocardium during tachycardia, which are two to three times that long.

In panel (a) an intracellular stimulus electrode, centrally located in the rectangle, depolarizes the nearby medium with effect that falls off radially from about four times diastolic threshold near the electrode to about half threshold near the medium's corners (see Appendix). With the rectangle uniformly set to the rest state (electrical diastole) just prior to the stimulus, the applied current depolarizes the stippled region, its border marking the locus of S = diastolic threshold. In terms of ventricular myocardium, the 24 mV threshold depolarization from resting potential is exceeded everywhere in the stippled area. The inner circle is the contour of critical local stimulus strength, $S = S^*$, inferred from the observed rotor positions. The unit of space was so chosen that the action potential propagates away from the circular border of the stippled disk at the standard 0·5 mm/msec myocardial speed. (Averaging 1/3 mm/msec across fibers and 2/3 mm/msec along the fiber orientation, we take 1/2 mm/msec as the speed of an uncurved front exciting completely recovered tissue). This simulation takes no account of non-uniformities of anisotropy, nor does it distinguish the distinct anisotropies of electrical conduction and of action potential propagation (Plonsey & Barr, 1984). The diagrams are drawn as though propagation were isotropic. By stretching them three-fold along one axis, they become accurate for uniform 3:1 anisotropy; there is no effect on temporal behavior.

Panel (b) schematically indicates the non-uniform initial condition actually used, in which an action potential entered the rectangle simultaneously along its ceiling, moved downward at 0.5 mm/msec, and exited through the floor. The horizontal line is the T^* isochronal contour moving downward at the same speed in the wake of that activation front. There is a vertical phase gradient, with the T^* locus in the middle of the rectangle, when the stimulus is applied at time 0 in the panel (b). The dots near the intersection of the moving T^* contour and the ephemeral S^* contour in panels (a) and (b) mark the eventual pivot points (phase singularities) of the mirror image pair of re-entrant vortices forming in the next 6 panels.

In panels (c-h) disks of diameter 15 mm are blackened around each pivot (and the outer circle shows its direction of rotation) to indicate the nominal vortex core,

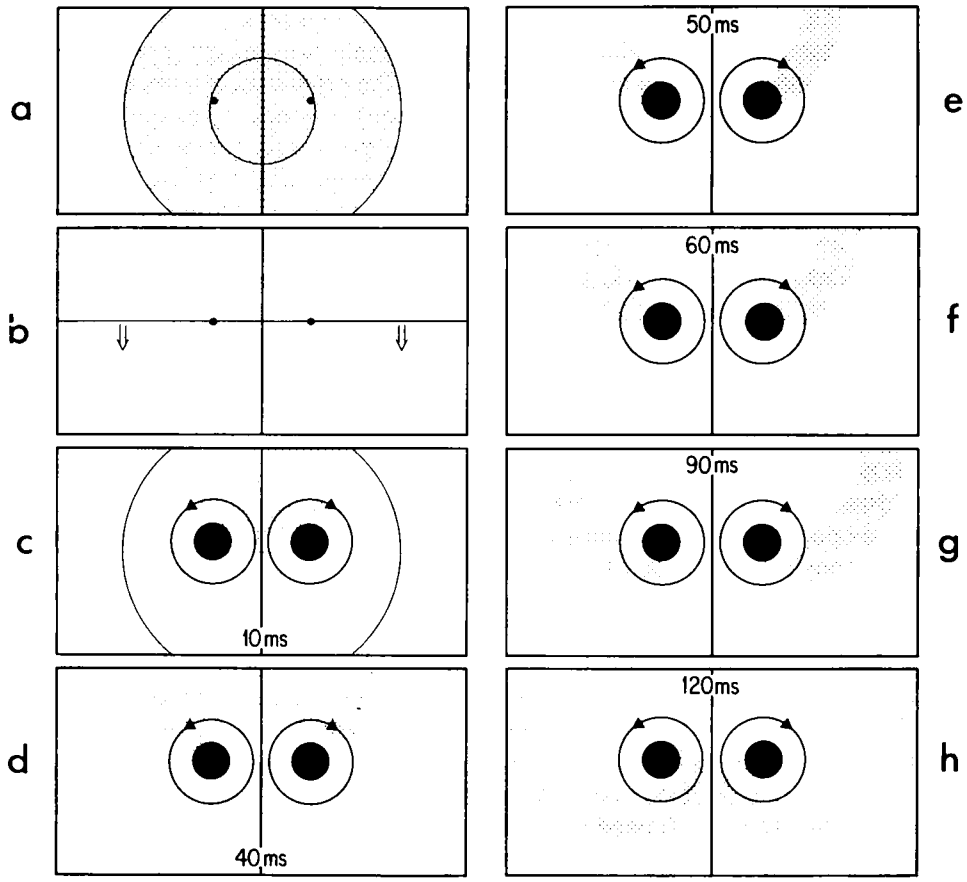

FIG. 12. Development of twin rotors, implemented in terms of a FitzHugh-Nagumo/cable-equation model for a 75 mm × 150 mm expanse of isotropic homogeneous excitable membrane. (If uniformly anisotropic, the picture is merely stretched along the fast axis.) The model is borrowed from FitzHugh (1961) with excitability slightly enhanced to support wave propagation, and with space and time scaled to match the propagation speed and vortex re-entry period experimentally observed in canine myocardium. In (a) a depolarizing current from the center of the rectangle achieves S = diastolic threshold along the outer circle, and $S = S^*$ along the inner circle; in (b) the stimulus was instead along the top edge of the rectangle, sending a wavefront from top to bottom of the rectangle with isochronal contour $T = T^*$ shown in its wake at time 0; in (c) stimulus (a) applied in situation (b) 10 msec previously initiated rotors around the two dots located in (a) and in (b) near the intersections of T^* with S^*; (d) through (h) show the development of paired spiral waves about mirror-image phase singularities within the black disks, at the times indicated. The layout of this pinwheel experiment follows the protocol of fig. 11 in Winfree (1985) and figs 6.1-6.5 in Winfree (1987).

a region of perimeter equal to the 47 mm wavelength (known from a separate, much longer, simulation) of the spiral wave beginning to shape up around it and radiate from it. In panel (c), 10 msec after the stimulus from the central electrode, only the stippled area inside the diastolic threshold circle is depolarized; the rest was too refractory (depending on distance ahead of T^*) to transgress the separator at the local stimulus strength (depending on radius from the central electrode). The

boundary of the immediately depolarized region in the 10 msec panel (c) marks the combinations of local T and local S (as on a strength-interval curve) which exceed local threshold. It is the geographical image of the separator in state space.

In panel (d), 40 msec after the stimulus, part of the boundary of the depolarized region has propagated in the direction shown by the arrows surrounding the black vortex cores. But part has not; in fact it has regressed. This was the region where local depolarization and refractoriness were both greatest, the upper right corner of Figs 2 and 5. As can be seen there, the membrane potential should come down promptly, and there is no nearby region of regenerative excitation. The boundary regresses.

The boundary between polarized and depolarized regions can move in either direction, depending on the local R. Where R is low, polarization changes to depolarization; where R is high, depolarization changes to polarization [see Fig. 2(a)]. R is low at the top of Fig. 12(b), but high near the T^* locus. When the low-R region is depolarized by the stimulus of Fig. 12(a), its boundary propagates outward; when the high-R region is depolarized, its boundary moves inward (Scott, 1977). In some excitable media repolarization may even actively propagate (Tyson & Fife, 1980; Tyson & Manoranjan, 1984). Whether this happens in cardiac muscle under physiological conditions is, I believe, still unknown. In any case, a place on the boundary of the depolarized (stippled) region between high and low R becomes a pivot. In the Russian literature this point is usually denoted as "q" (Gulko & Petrov, 1972; Zykov, 1984, Figs 5.1-5.3). I refer to it as a "phase singularity" since the periodic excitation felt throughout the medium turns on that point and its amplitude falls there to zero.

This failure of the boundary to propagate in the direction naively expected (outward from the depolarized region) might be called "unidirectional conduction block", a feature often said to be the *sine qua non* of re-entry induction (e.g. Berne & Levy, 1983; Gough *et al.*, 1985; Kadish *et al.*, 1988). In section 3.2.2 above I proposed a different interpretation.

In panel (e), 50 msec after the stimulus, the regressing part of the initial border has become the backside of a potentially re-entrant wavefront. This front follows the descending T^* locus until 120 msec, when it breaks through the original stimulus site in a direction opposite to that of the original activation front, thus completing re-entry. From Fig. 2 it is easy to appreciate that at the point closest to the stimulus source along the T^* locus, the re-entrant wave must move opposite to the wave that established the original phase gradient. Whatever timing gradient may have existed there just prior to the inducing stimulus, it mapped that region to state space as in Fig. 2(a): along the final approach to rest, with some parts further along than others. Elevated to maximum depolarization after the stimulus, this region's image remains the same but the parts that were more advanced along the bottom of the loop trajectory are now the laggards along its top: the region's gradient is now pointed backward along the cycle.

This vortex continues to rotate at 120 msec period, with wavespeed (47 mm/120 msec = 0.4 mm/msec) somewhat reduced from that of a solitary uncurved action potential. The speed is reduced by outward curvature of the front (the major

factor in this case) and by lingering refractoriness of the medium into which the front propagates (a relatively minor factor in this case). The shape of the spiral wavefront and its period of circulation are here determined mainly by the dependence of speed on curvature (Zykov, 1984; Keener, 1986; Keener & Tyson, 1986; Tyson & Keener, 1987, 1988), which is determined mainly by the mechanisms of excitation, as distinguished from the mechanisms of late refractoriness. With the particular parameters adopted in this simulation, the refractory period plays little role: it is less than 70 msec (measured in separate simulations by applying stimuli in the wake of a one-dimensional propagating pulse) but the two-dimensional circulation period is 120 msec, leaving a wide excitable gap ahead of the wavefront. The periodic pulses emanating from the rotor are spaced 47 mm apart, but as the interval between successive pulses is shortened their propagation speed falls off smoothly from 0·5 mm/msec (solitary pulse) to 0·4 mm/msec (rotor) to 0·3 mm/msec at a critical minimum distance near 25 mm (period then near 80 ms), at which point propagation fails. Waves at longer periods are perfectly stable if their fronts are not curved. It will be of interest to examine the excitable gap in quantitatively more realistic models of myocardial excitability, because the gap is thought to be quite small in "leading circle tachycardia" (Allessie *et al.*, 1977; van Capelle & Allessie, in press). I use the vaguer concept "vortex" rather than "leading circle" because the latter entails specific features that are not generic to the rotors computed by myself and many Russian biophysicists since the early 1970's. The leading circle is a one-dimensional closed-ring circuit along which "the stimulating efficacy of the circulating wave-front is just enough to excite the tissue ahead which is still in its refractory phase", with the consequence that there remains no excitable gap (Allessie *et al.*, 1977). In generic vortex reentry there seems to be no distinguished circuit. There usually is a substantial excitable gap since the wavefront generally cannot curve sharply enough to circulate as quickly as cells can recover. And the concept of "refractory period" is relatively useless because both excitation and recovery processes are distorted at these short periods. Numerical experiments on more realistic cardiac membrane models will reveal whether they behave more like the "leading circle" model than is generically the case.

This rotation is not quite rigid: the nominal pivot itself traverses a tiny circle in a time several-fold longer than the spiral wave's period. The inner tip of the spiral wave thus traces out a very regular pattern of loops organized around a center. With the particular parameters used in this simulation the path resembles a flower with eight petals (Fig. 13), but the path does not close and the "number of petals" is not an integer. It is determined by the ratio of two periods, both of which vary continuously but independently with the parameters describing the medium. Such "meander" (Winfree, 1973) has turned out to be typical of rotors in numerical excitable media (see references in Winfree, 1987, p. 181; Zykov, 1986, 1987; Jahnke *et al.*, 1989) except that it is not so irregular as I believed when affixing the name "meander" to it. Very regularly periodic meander has been observed in chemically excitable media (Winfree, 1987, Fig. 7.16; Jahnke *et al.*, 1989). According to Zykov (1984) it is also characteristic of normal myocardium. Numerical simulations of van Capelle & Durrer (1980) show it (see Winfree, 1987, fig. 5.3) in a model of

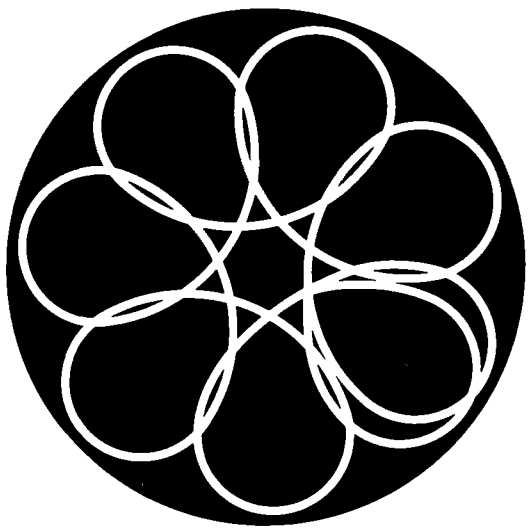

FIG. 13. Isochronal contours often cannot be projected all the way to a center of rotation, because the activation wavefront ceases to be normal some mm short of that terminus: the wavefront's tip orbits around a temporary center which is itself more slowly following a circular path, so that the wave tip describes flowery loops. The white tracing is a 1 sec segment of the (non-closed) path of the wavetip in the FitzHugh-Nagumo model with parameters as in Figs 12 and 14. To provide a size scale, the black disk represents the 15 mm rotor indicated in black on Figs 12 and 14. The path of the temporary pivot (not shown) is a circle about 9 mm in diameter through the centers of the eight loops, traversed in slightly less than 1 sec. Although these "flowers" are seldom bigger than the rotor in normally excitable media, they become much larger in less excitable media which might model depressed, ischemic, myocardium: the center of reentry meanders through such medium in ways that might resemble *torsade de pointes* on an electrocardiogram.

myocardium similar to the one used here. We have observed it also in rotors computed using Beeler-Reuter membrane coupled via the cable equation. Seen through the electrocardiogram, a widely meandering rotor in myocardium might resemble *torsade de pointes*, since the direction from which activations predominantly approach the pickup electrode would change periodically on a time scale of many rotations while the vortex moves throughout the ventricles.

The various panels of Fig. 14 show what happens if the stimulus, I, is given at a different moments, CI, during the vulnerable period, starting (first panel) at a time ("0 msec") when the two intersections are about far enough apart to permit stable coexistence of two rotors. Each panel depicts the medium 120 msec after the stimulus (on its first anniversary at the period of the tachycardia). The third panel ("16 msec") is the last panel of Fig. 12. Each panel shows the T^* and S^* contours at the moment of stimulation: their intersection is always close to the pivot (the phase singularity) of the vortex core that eventually forms nearby. To first approximation the locus of pivots follows the S^* contour.

By changing stimulus current rather than coupling interval, the intersections are displaced (as the S^* circle changes diameter) roughly along the T^* isochronal

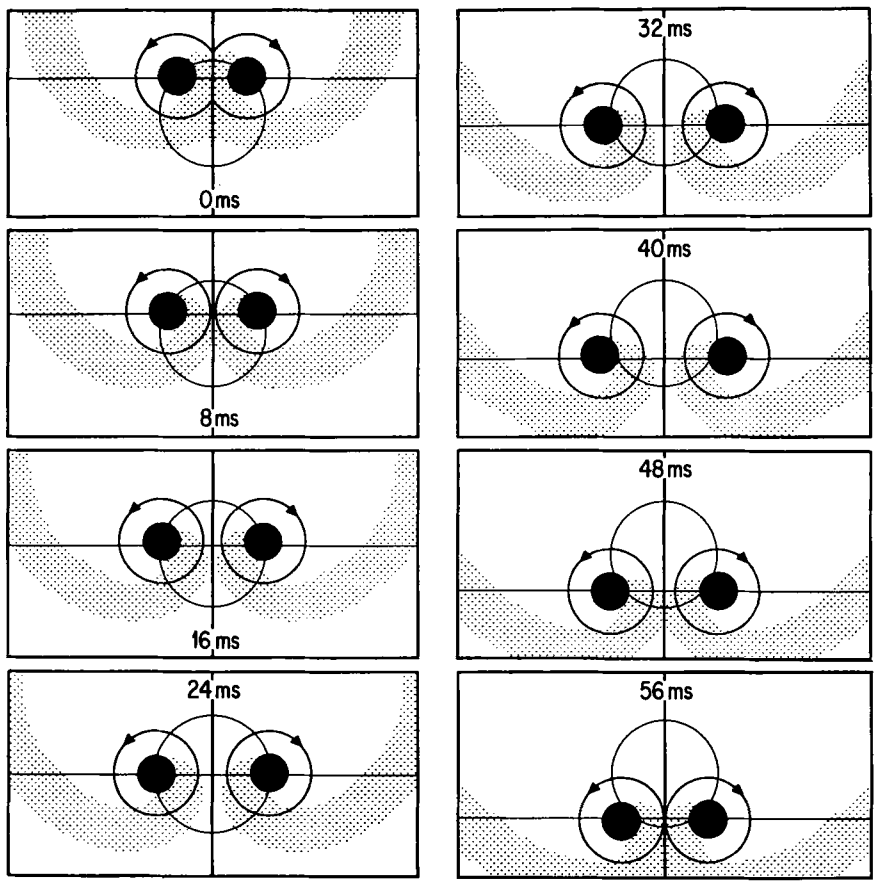

FIG. 14. In each panel twin rotors are shown at the same age as in Fig. 12(h) (120 msec = only one rotation period after the premature stimulus), but in each of eight otherwise identical experiments started later and later in the vulnerable period, from a moment almost too early to achieve intersections (here called time 0), until a moment almost too late (56 msec later). In each panel the T^* isochronal contour and the S^* critical stimulus locus are shown where they were when the premature stimulus was given 120 msec previously. These spiral waves are only beginning to form: they wrap tighter during the next few rotations (not shown). The "16 msec" panel is Fig. 12(h).

contour (computations not shown). This numerical experiment has been replicated in canine myocardium, as noted below (Frazier *et al.*, 1989).

By making the stimulus negative (hyperpolarizing rather than depolarizing, as if applying a quick pulse-chase with acetylcholine rather than extracellular current) one obtains rotor pairs just as above (computations not shown). As in Figs 7.13–14 of Winfree (1987), in this numerical experiment T^* occurs during the depolarized phase of the action potential. The hyperpolarizing S^* is about the same strength as the depolarizing S^*, being about half the vertical dimension of the excitation-recovery loop at that T. But instead of an island of depolarization around the simulus center, we have an island of enhanced R, of refractoriness: the $S = S^*$ ring produces "an arc of unidirectional conduction block". If this island vanishes while interrupting

a passing wavefront, twin rotors are left in its wake. This version of the numerical experiment more resembles the spontaneous apparition of "figure-eight reentry" when activation fronts encounter islands of tissue with intrinsically lingering refractoriness (Allessie *et al.*, 1977; Boineau *et al.*, 1980; Gough *et al.*, 1985; El-Sherif, 1985.)

The FitzHugh–Nagumo/cable equation model cannot provide a quantitatively reliable caricature of myocardial electrophysiology. This already seemed likely when I started this project three years ago, and became quite clear a year later when the numerical results were plotted. For example ventricular membrane, unlike squid axon, has *two* excitability mechanisms, a fast one involving sodium (as in the Hodgkin–Huxley and FitzHugh–Nagumo descriptions of squid axon) and a slower one involving calcium (thought to be responsible for "slow waves" (Berne & Levy, 1983). Unless these two mechanisms happen to stay synchronous, a usable myocardial membrane model must need *two* distinct "*R*"*s* rather than the one supposed to represent overall recovery of excitability in the FitzHugh–Nagumo model or any other two-variable caricature of the membrane. Zykov's description of myocardial membrane based on a 1962 Purkinje fiber model of Noble (Zykov, 1984) represents an advance over the 1961 FitzHugh–Nagumo model, but having no explicit calcium process, and being reduced finally to two variables, it also must make contemporary electrophysiologists uncomfortable. So the FitzHugh–Nagumo generic membrane was replaced in these computations by the Beeler–Reuter model of space-clamped mammalian ventricular myocardium (Beeler & Reuter, 1977).

Space-clamped excitation and recovery in this implementation of the Beeler–Reuter model agrees in detail with published accounts of the same computations and with the time-course of membrane potential in real fibers. Its integration into the spatial context was handled by the cable-equation algorithm previously tested in detail. Being unsure how to scale space in these two-dimensional computations, I again adopted a unit of space so that the speed of the computed action potential is 1/2 mm/msec. Now we can ask: "Does the Beeler–Reuter membrane support two-dimensional vortex-like reentry?" It does, but its sodium and calcium excitations do not stay synchronous after the onset of tachycardia: in some places at some times, the sodium channels open abruptly as in a normal action potential but the calcium channels still remain refractory. This sodium front propagates at the normal speed, but regions thus excited recover more quickly (60–70 msec) than they would had calcium excitation also occurred (200–280 msec). The sodium front can fragment upon encountering islands of refractoriness still kept depolarized by the calcium channels excited during the prior excitation. Perhaps because of this dissociation of the two excitation mechanisms that couple through membrane potential, the vortex center wanders and its wavefronts break, nucleating new re-entrant vortex pairs which also wander (Fig. 15). This resembles epicardial maps of the earliest stage of fibrillation, but the period is too long. Tachycardia computed in 2-dimensional reentry never has a (poorly-defined) cycle time less than about 200 msec. In contrast, the analogous vortices in dog myocardium spin regularly once every 100–120 msec, and during such frequent re-excitation the myocardial refractory period may be as short as 70 msec (Janse *et al.*, 1969; Chen *et al.*, in press). The Beeler–Reuter vortices do spin in the simple way familiar from models like FitzHugh–

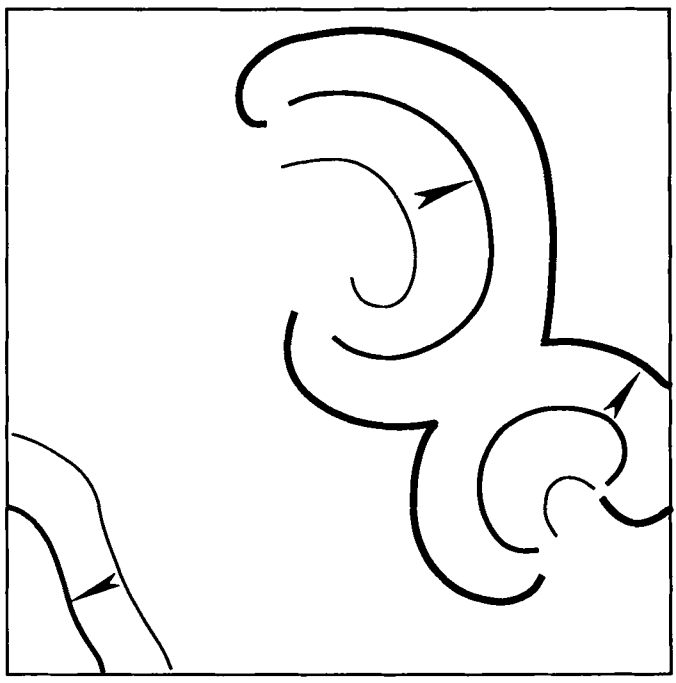

FIG. 15. The Beeler-Reuter model of ventricular membrane replaced the FitzHugh-Nagumo model in a two-dimensional cable-equation medium. With appropriate initial conditions, it also supports reentrant vortices. Arcs of undirectional conduction block arise unexpectedly, creating new endpoints, each of which also wanders more freely than in FitzHugh-Nagumo calculations, probably because the dual excitability mechanism of this more elaborate model. Several extra vortex pairs arose during this computation, some pairs vanished by mutual annihilation, and one solitary vortex vanished into the adjacent wall, leaving only two pairs at the moment shown. In this snapshot wavefronts are indicated (thicker and thicker at successive 40 msec intervals) on a square of 200×200 cells, with cells about 600 μ apart, 840 msec after initiating a single rotor, with $[K_0]$ in the intracellular clefts elevated from normal 3·5 mM to 7 mM as a consequence of rapid pacing (Mogul *et al.*, 1984).

Nagumo if the simulated calcium current (which is well known to need major revisions) is artificially attenuated or eliminated altogether. In this situation there remains only the single excitability process mediated by sodium and potassium channels, much as in FitzHugh-Nagumo membrane. The vortex reentry period then shortens to somewhat less than 120 msec, close to the experimentally observed period. It may be of interest in this connection that Dillon & Wit (1988) report that a calcium channel blocking agent had no effect on their ability to induce or terminate re-entry in isolated rabbit hearts.

The opposite situation is common in ischemic tissue: the resting potential is relatively depolarized, so sodium channels are inactive and excitation is not affected by the sodium-channel blocker, tetrodotoxin; excitation is carried by the calcium process and is eliminated by the calcium channel blocker, verapamil (Akiyama, 1981). We were unable to sustain vortex reentry in the Beeler-Reuter model in the absence of sodium channels, but this may reflect only our failure to contrive appropriate initial conditions, or the coarseness of these first simulations.

We did not examine the Beeler-Reuter vortex for an excitable gap or establish whether its period is determined mainly by the dependence of front speed on curvature (and thus by sodium channel kinetics) or mainly by refractoriness (and thus additionally by potassium and calcium channel kinetics). This preliminary investigation was very expensive in computer time and needs to be repeated with several-fold finer mesh.

The Beeler-Reuter model's vintage-1977 ionic mechanisms have been superseded by more recent electrophysiological experiments, so the DiFrancesco-Noble model of Purkinje fiber (DiFrancesco & Noble, 1984) in FORTRAN was implemented as a more modern replacement for the FitzHugh-Nagumo model. This implementation is again in exact correspondence with published results [except for Fig. 12 of DiFrancesco & Noble 1984, which was in error (D. Noble, personal communication)]. But simulated Purkinje fiber action potentials propagate one-dimensionally at a speed that still requires correction by an otherwise arbitrary factor, and there is not yet a published adaptation appropriate to ventricular myocardium.

Computations, of course, do not tell us whether the dual excitability mechanism of myocardium during reentry maintains the synchrony implicit in using the FitzHugh-Nagumo metaphor. If, as in the Beeler-Reuter model, sodium excitation occurs sometimes with and sometimes without calcium excitation during reentrant tachycardia, then the FitzHugh-Nagumo numerical experiments emphasized in this paper may thus be limited to interpreting the *onset* of reentrant tachycardia in ventricular myocardium.

Why then do I exhume this old (1986) attempt design myocardial pinwheel experiments using the generic FitzHugh-Nagumo model? Because attempts during the past two years to improve the quantitative agreement by deploying more elaborate membrane kinetics (Beeler-Reuter, DiFrancesco-Noble) have in fact not superseded this vintage-1986 "rough draft"; if short-period reentrant tachycardias consistently fail to excite the myocardial calcium mechanism, then the FitzHugh-Nagumo caricature may even be more appropriate. The modeling can be refined in many obvious ways; but it has also become obvious that it will be enormously more complicated before its quantitative accuracy is substantially improved. So the conceptual design of the pinwheel experiment may remain most transparent in the present terms.

A second reason for presenting this simple theoretical framework is the recent publication of laboratory experiments validating its qualitative predictions.

5. The Pinwheel Experiment in Canine Ventricular Myocardium

(5.1) TESTABLE INFERENCES

The main conclusions from sections 2-4 which differ from the conclusions of more familiar schemes are:

(i) Isochronal contours can be confluent to a pivot, a phase singularity. They need not terminate discontinuously along a transverse "arc of conduction block". (Qualifications: so long as "meander" persists, each new isochronal contour terminates at a more advanced position along the path of the moving

pivot; and in strongly anisotropic media such as epicardium surviving over an intramural infarct, coarsely sampled contours may give the appearance of convergence to a line-segment rather than to a point.)

(ii) A phase singularity appears close to the intersection of two critical contours existing at the moment a discrete stimulus ends:

(a) A contour of critical local phase, T^*, which, *only* for depolarizing electrical stimuli, lies somewhere near the end of the refractory zone, under the interior of the excitation-recovery loop of Fig. 2; and

(b) A contour of critical local stimulus strength, S^*, defined to correspond to the local stimulus requirement for moving membrane potential into the middle zone of the excitation-recovery loop at phase T^* in Figs 2 and 5 (supposing S purely depolarizes). In the numerical model of Fig. 12, S^* is about twice the diastolic threshold, or about one third of the peak-to-peak amplitude of the action potential. In good approximation S^* could probably be read from a strength-interval curve measured in living membrane stimulated in the same way, if T^* were known.

(c) Constancy of the putative T^* and S^* among diverse situations should be checked as follows. Having located a rotor experimentally, follow the band of iso-S contours and the band of iso-T contours which it straddles. If they cross again, there should be another rotor there, its handedness determined by the direction of crossing. And in a series of experiments varying CI or I, see whether the same bands are implicated.

It is clear from simulations that the final position of the rotor's pivot in relation to the intersection of nominal T^* and S^* contours is affected by the initial shapes of the T and S gradients nearby. Experiments are needed to determine how large this effect is, and so how useful is the "T^*, S^*" rule of thumb. (See corresponding item section 5.2 below.)

(iii) Transversal crossing is necessary to evoke vortex reentry; where contours are tangent nothing should happen.

(iv) Given prior activation by a broad wavefront whose passage created a phase gradient, and a central maximum of stimulus strength, these contours will resemble a line and a ring, respectively, and they will cross twice, creating mirror-image phase singularities.

(v) "Phase singularity" is only a mathematical abstraction signifying the pivot point of a rotor. The region covered and/or enclosed by the rotor in its path around the singularity has finite diameter which can be estimated numerically (given an adequate electrophysiological model of the membrane); in Figs 12–14 it is about 15 mm.

(vi) Only stimuli within a compact domain of coupling interval and current combinations will evoke persistent rotors and—perhaps—fibrillation. Surrounding this bull's-eye on all sides is an annulus of stimulus combinations that evoke only a short run of repetitive responses:

(a) Delivering the stimulus at later and later coupling intervals, CI, will cause the twin intersections to scan across the S^* ring, defining a vulnerable interval. In the middle of this interval the rotors are far apart

and persist through many rotations, but at the extremities they are adjacent or overlapping and so cancel one another after one or a few ectopic beats.

(b) Increasing the stimulus current, I, through a minimum will cause the S^* contour first to appear at the electrode tip, then grow to a tiny ring, admitting the possibility of overlapping rotors and repetitive extrasystoles. Above that I, stable rotor pairs can be created which may induce fibrillation. Near a certain maximum I the entire medium has $S > S^*$ so it is no longer vulnerable. Approaching this extreme, the only possible rotors are close together or near a tissue boundary, resulting in only a few ectopic beats.

The classical interpretation of vulnerability to a premature stimulus in myocardium focuses on non-uniform dispersion of refractoriness as the cause of conduction block, and infers that this combination is the *sine qua non* of fibrillation—or, sometimes, also of electrically-induced reentry *leading to* fibrillation. Yet the theoretical approach reviewed above made no use of fine-scale heterogeneity, and inferred electrophysiological phenomena which are not to be found in textbook discussions of vulnerability. Reasonably enough, for several years these inferences seemed to the few physiologists approached unworthy of testing. This situation changed during 1985–1988 when their own investigations into defibrillation led R. E. Ideker and students to execute the critical experiments in canine ventricular myocardium.

(5.2) TESTING IN NORMAL, UNDAMAGED DOG MYOCARDIUM

These experiments are simple in concept but exceptionally complex in execution; they require meticulous attention to details of the dog's physiological condition, of the millisecond-scale workings of on-line electrical recording devices, and of the digital recording and analysis of data (Ideker *et al.*, 1987; Witkowski & Penkoske, 1988*a*,*b*). Interpretation is subject to more qualifications and provisos than could be written on this page.

For example, there is the interpretation of "stimulus". In the context of electrophysiological theory it can only mean intracellular current or membrane potential displacement. "Local stimulus strength" is thus a reasonably clear idea when we are discussing an isolated cell membrane. However in the case of the intended experimental application, the stimulus is an extracellularly-provided current that penetrates a tissue composed of membrane wrapping diversely oriented cylindrical fibers, which are irregularly joined by low-resistance junctions. Thus, current runs in and out of the membranes at all angles, at diverse current densities: from the viewpoint of microscopic theory, the situation is hopelessly complicated. However behavior on the scale of millimeters to centimeters seems dominated by whatever few small patches first exceed threshold for depolarization. Making this idea more quantitative, Chen *et al.* (1986*a*) and Frazier *et al.* (1988*a*) have shown that extracellular current has a net depolarizing effect on bulk tissue, achieving diastolic threshold at 3 msec × 50–100 mV/mm of external potential gradient (depending on fiber

orientation). Were membranes merely stacked as in a battery, this would correspond to only a few mV (positive or negative depending on membrane polarity) per membrane crossed perpendicularly, and less for those crossed obliquely (Winfree & Guilford, 1988). The actual mechanism presumably involves extreme heterogeneity of current flow so that just *some* patches of membrane are depolarized by more than the 24 mV required to trigger normal myocardial membrane from rest.

Similar complications attend the extracellular identification of action potential complexes, especially near a convergence of isochronal contours where conduction is slow and complexes abnormal. Use of bipolar electrodes makes it impossible to detect broad regions of simultaneous depolarization or wavefronts arriving from certain directions. Other difficulties surround the interpolation of isochronal contours in two or three dimensions, and so on. A proper abstract of the results from the several pertinent papers would be a whole new paper by itself. For the present, the only thing to do is to read the originals. Here I simply cite them and extract or quote from the overall conclusions as they pertain to the points listed above:

(i) Until quite recently the convergence of isochronal contours to a point-like phase singularity was not supported by any published isochronal maps. The isochronal contours are all sketched to show arcs of strict discontinuity in event timing (and so in membrane potential), referred to as "conduction block" (e.g. El-Sherif *et al.*, 1981; Mehra *et al.*, 1983; Gough *et al.*, 1985; El-Sherif, 1985; Cardinal *et al.*, 1988; Chen *et al.*, in press; Shibata *et al.*, 1988; Frazier *et al.*, in press). However the isochronal contours do converge in pinwheel fashion toward that arc, and its length seems to diminish as instrumental resolution improves, only a few mm remaining in some cases. The interpreted length is proportional to the assumed minimum speed of slowly propagating action potentials; this limit also seems to be falling. Dillon *et al.* (1988) for example, accept 0.05 mm/msec, which puts the few mm of residual arc length almost at the resolution to extracellular mapping technique today:

> "The lines of apparent block during sustained tachycardia can be distinguished from the lines of real block that occur during initiation of tachycardia by premature impulses ... reentry is most likely occurring around a small central fulcrum rather than around long lines of block..." (Dillon *et al.*, 1988).

The residual arc length may turn out to be a consequence of meander. In Fig. 16 contours are redrawn through published data to show compatibility with a point-like convergence.

(ii) The consistent apparition of the phase singularity near the intersection of critical contours in an appropriate context was confirmed in good approximation by Frazier *et al.* (1988*b*) and by Shibata *et al.* (1988) using canine left and right ventricles: "... reentry occurred where cells were in a particular stage of recovery and the potential gradient field created by the shock was in a particular range of strengths. ...". More quantitative follow-up in the same laboratory (Frazier *et al.* 1989) refined the electrode arrangements for this pinwheel experiment to set up the strictly orthogonal gradients used numerically (Winfree, 1974*a*,*b*). In this arrangement the critical S^* (the iso-S contour of the pivot of the reentrant vortex) was found to be 5 msec * 400 to 600 mV/mm extracellular in canine myocardium

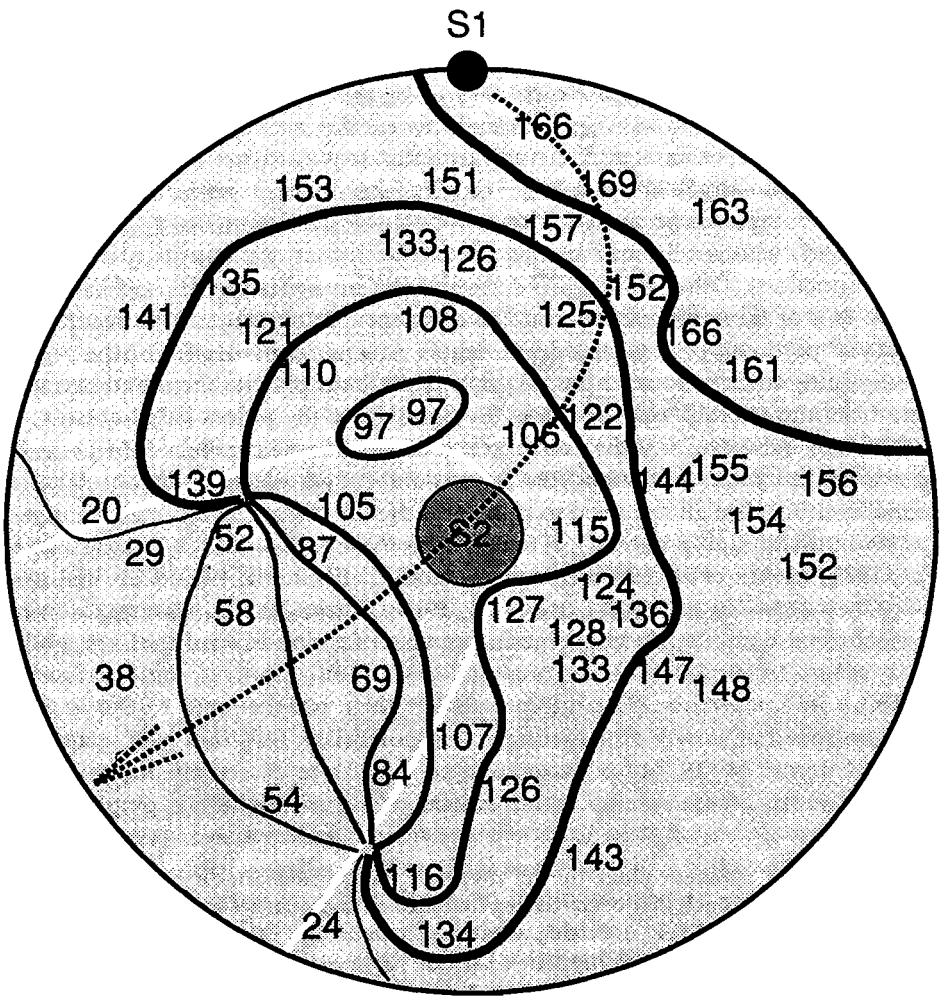

FIG. 16. On a polar projection of the canine ventricular epicardium similar to Fig. 4 or Figs 9-11, isochronal contours are sketched as in Fig. 1 (bottom). The data points (numbers: local activation time in msec after $S2$ stimulus) are from fig. 5F1 of Shibata *et al.* (1988); the contours are here resketched rather differently through the same data. The right-ventricular $S1$ electrode at the top (black disk) sent an activation wavefront from top (posterior left ventricle) to bottom (anterior right ventricle) roughly as indicated by the dotted arrow, establishing a T field that is somewhat more curved than in Fig. 9(a) and conspicuously concave in this projection. The apical $S2$ electrode (larger gray disk) was fired when fibers along the white band were near $T^* = 145$ msec after local activation. The thinnest contour is hand-sketched through electrodes that detect an activation front about 20 msec later; successively thicker contours are sketched 20 msec apart up to 160 msec. The 140 msec contour occupies nearly the same places as did the 20 msec contour. As in Figs 12 and 14, activation continued to rotate counterclockwise on the left (posterior right ventricle) and clockwise on the bottom (anterior right ventricle) at 100-120 msec intervals, but in real myocardium it then degenerated to fibrillation.

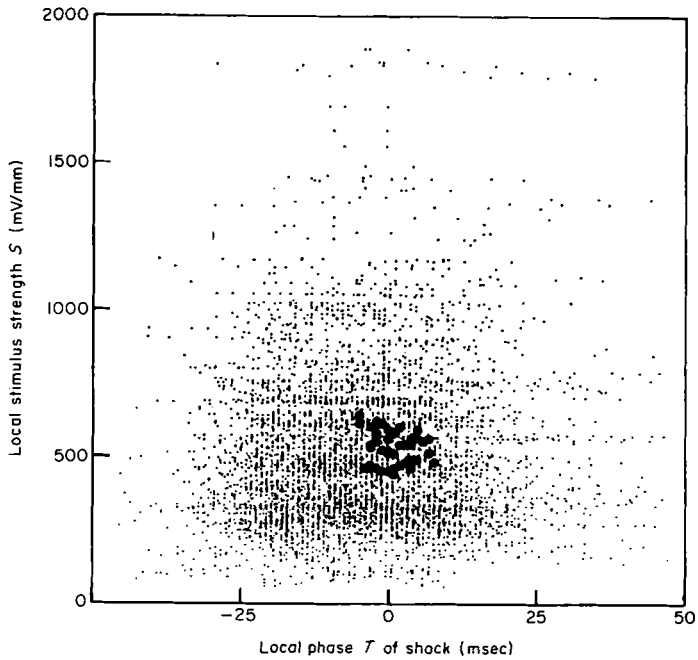

FIG. 17. Each dot represents the local stimulus strength S (measured by the local extracellular potential gradient, vertically) and local phase T (measured in msec from a zero at the moment when the local tissue recovers excitability to a standard test stimulus) when that stimulus arrives at the site of an electrode, in data pooled from experiments on the ventricles of 11 dogs. If a re-entrant vortex arises with its pivot near the electrode, the dot is enlarged. Large dots are found only within a 30 msec range of T and only where S lies between 400 and 600 mV/mm, thus estimating T^* and S^*. (Adapted from Fig. 8 of Frazier *et al.*, in press.)

(averaging over all fiber orientations) (Fig. 17). This is five to seven times the diastolic threshold. If threshold is reached when some microscopic hot-spots in the spongy cardiac membrane exceed 24 mV depolarization, then S^* corresponds to exceeding 120–168 mV depolarization (more than reached in a full action-potential) at those hot-spots, and lesser depolarizations presumably ranging to 120–168 mV hyperpolarization, at other spots on the membrane. (This seems at least double the estimate obtained from the FitzHugh–Nagumo simulation.) The outer ring of $S =$ diastolic threshold would have been far outside the medium in the experiments of Shibata *et al.* (1988), which used such a strong apical shock that the entire myocardium depolarized. The critical T^* in this situation (Frazier *et al.*, in press) varies from 129 to 179 msec, but stays within a range spanning less than 30 msec around the refractory period as assayed by a 2mA stimulus of 3 msec duration. It should be noted that the notion of a "refractory period" has limited utility in this context, beyond providing a standard state as a timing reference: it varies widely according to manner of assaying stimulation and recent history of stimulation. For example, during 100–120 msec vortex re-entry in healthy myocardium the refractory period may be as short as 70–80 msec (Chen *et al.*, in press).

Explicit fulfillment of testing protocol (c) above depends on seeing the iso-S contours, but they are not available in Shibata *et al.* (1988) or in Chen *et al.* (1988). Comparison with iso-S data in Chen *et al.* (1986*a*) allows only a very rough check for constancy of T^* and S^* in the Shibata *et al.* (1988) experiment. The hundreds of small dots in Fig. 17 show combinations of T and S achieved in the pinwheel experiments of Frazier *et al.* (in press); the few large dots characterize the sites of rotor pivots. They are tightly clustered.

(iii) Preoccupation with "critical" T and S values should not be allowed to obscure the context of their utility: rotors develop where a *gradient* of T crosses transversely through a *gradient* of S. The values of T and S spanned must not fall far short of requirements for stretching the medium's image fully over the excitation-recovery loop. To do so it is necessary but not sufficient that they straddle T^* and S^*: the range of T and S must also be sufficient, and the gradients cannot be parallel. Frazier *et al.* (in press) tested this extreme case and found that the same gradients that otherwise elicit rotor pairs *do not* if they are arranged to run antiparallel rather than orthogonally.

(iv) The creation of rotors in mirror-image pairs under carefully arranged circumstances was confirmed (Chen *et al.*, 1988, using canine right ventricle):

> "We wanted to test the prediction of a new explanation for the mechanism of the electrical initiation of VF proposed by Winfree ... he predicted that a pair of singularity points will be present and cause two mirror-image rotors that will form a figure-of-eight re-entry pattern as we observed experimentally ... a three-dimensional figure-of-eight re-entry pattern is the mechanism of ventricular vulnerability ... "

and (Shibata *et al.*, 1988, using ventricularly paced canine left and right ventricles) (Fig. 16).

> "Winfree has predicted that this special situation should lead to two re-entrant loops circulating in opposite directions, one in each of two regions. We observed such re-entrant loops in this study."

(v) The vortex core diameter was estimated: Chen *et al.* (1988) observed stable mirror-image vortices as close together as 12 mm in the canine right ventricular infundibulum.

(vi) The bull's-eye target on the vulnerability diagram was densely sampled. The phrase "upper limit of vulnerability" was coined by Ideker & Shibata (1986) and Chen *et al.* (1986*a*) in the course of experimentally testing this prediction (then discovering a prior experimental demonstration by Fabiato *et al.* (1967) and by Lesigne *et al.* 1976). (Shibata *et al.*, 1988, using canine ventricle normally paced endocardially by sinus node through Purkinje fibers) (Fig. 18):

> "An upper limit to the energy of shocks that induced ventricular fibrillation was found for all coupling intervals tested. Thus, a plot of the vulnerable period on a strength-interval graph is closed rather than open at the top. This vulnerable region is surrounded in many areas by shock strengths and intervals that give rise to repetitive responses ... This finding was predicted by Winfree from topological considerations. Repetitive responses occurred on all sides of the vulnerable region, including the top, as was also predicted by Winfree."

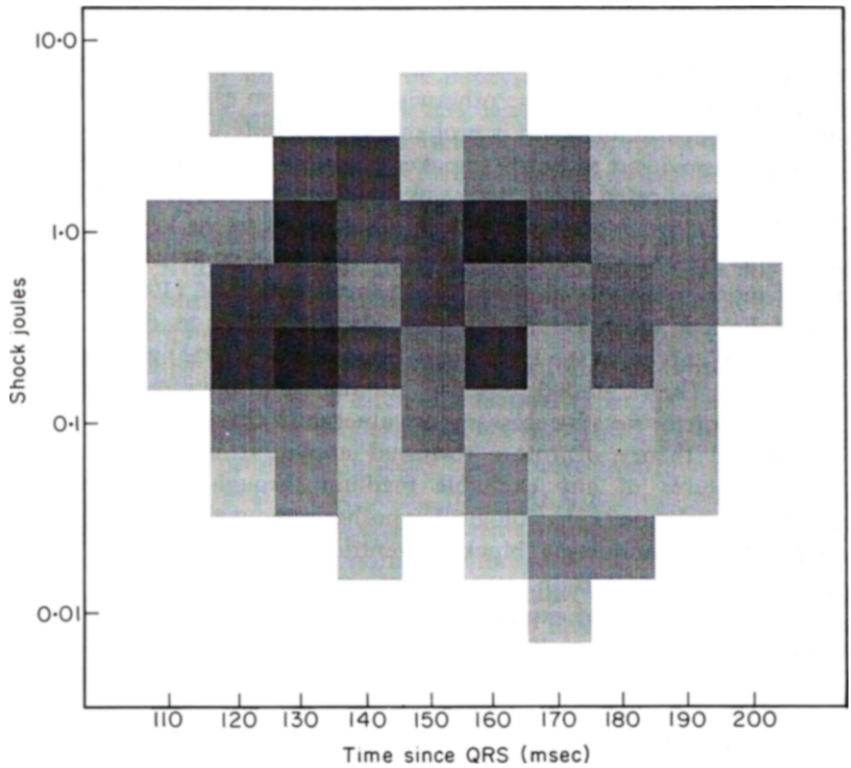

FIG. 18. Using darkness proportional to the percentage of fibrillation episodes in many pooled dog experiments, the vulnerable domain is seen as a compact island surrounded by stimulus (timing, current) combinations that never evoke fibrillation (white). Adapted from Shibata *et al.* (1988), table 2.

In short, pinwheel experiments using healthy dog hearts confirm the foregoing expectations based on the analogy to generic excitable media:

> "Winfree has made four predictions . . .

[same ideas as repackaged above]

> We performed a series of experiments to test these predictions . . . all four predictions were correct. Thus application of the concept of phase resetting to cardiac dysrhythmias has led to the prediction of four electrophysiologic phenomena that were not previously known and have now been experimentally confirmed." (Ideker & Shibata, 1986).

(I must add that I consider the emphasis on phase resetting misplaced. I presented the theory in those terms in Winfree (1983, 1987) in an attempt to communicate without using the original and, in my opinion, more correct concepts of Winfree (1973, 1974*a*,*b*, 1978), because the latter apparently have less intuitive appeal to others than to me. I see the phase resetting concepts as a crude one-variable analogy (Winfree, 1987, appendix) to the two-variable or n-variable reality of excitable media, to which earlier paradigm I revert in this paper.

(5.3) CONCLUSION FROM THESE INITIAL EXPERIMENTAL TESTS

This perspective on cardiology from the viewpoint of the dynamics of generic excitable media has grasped some otherwise unforeseen essentials of the behavior of ventricular myocardium. But it is probably not the *only* way to think about these things. It just turned out to be the quickest shortcut through a lot of physiology that proved so complicated that nobody saw their way through it before. In particular, the "phase" model led more directly than other routes to the key inferences. Now that the results are known, physiologists may wish to reconstruct these inferences in terms of more conventional concepts. In fact Chen *et al.* (1988), Shibata *et al.* (1988) and Frazier *et al.* (in press) have already begun to do so in terms of strength-interval curves, in the tradition of Brooks *et al.* (1955) and Foy (1974, pp. 84–78, 255–256). Their "graded response" alternative to the idea that non-uniform dispersion of refractoriness is necessary for vulnerability to reentry is a verbal version of the standard theory of rotors reviewed above. It introduces the intrinsic geometrical features of any excitable medium through a supplementary (or equivalent, in translation?) physiological hypothesis about abortive action potentials and unidirectional conduction block in ventricular myocardium in response to electrical stimulation of certain intensities at certain phases.

Regardless of the style of explanation preferred, it will be necessary to sharpen hypotheses involving "non-uniform dispersion of refractoriness" as the necessary and sufficient condition for vulnerability, also distinguishing vulnerability to fibrillation from vulnerability to reentry. There are at least two possibilities:

(i) retain only the hypothesis of Moe (1962) and Moe *et al.* (1964) about micro-reentrant fibrillation after the onset of reentry, abandoning the apparently incorrect idea that non-uniform dispersion of refractoriness is essential also for the onset of reentry; or

(ii) retain the vaguely statistical meaning of "dispersion of refractoriness' for infarcted and ischemic myocardium but redefine it as regards the undamaged tissue addressed in this theory and these experiments to *mean* the orderly ephemeral gradients here described. The distinction between permanent (parameter) and ephemeral (state) gradients has been poorly maintained in the literature. It was not necessary or possible to make a distinction between disorderly and orderly gradients before the recent advent of high-resolution mapping instruments.

This question is discussed further in Frazier *et al.* (in press), Ideker *et al.* (in press) and in Winfree (1982, 1986*b*, 1989*b*) with suggested relevant experiments.

6. Conclusion

Excitable media have certain characteristic behaviors, including 2-dimensional and 3-dimensional rotors that drive the medium into regularly periodic activity. Some of the essential behavior can be guessed by attending to the topology of phase singularities in periodically active media. Much of it can be understood by just thinking about the intersections of two kinds of observable critical curves. Decisive

experiments were designed some years ago to look for the otherwise unforeseen phenomena predicted from this unorthodox perspective. They have since been found in cardiac muscle. They now need to be understood in quantitative terms of the specific mechanisms of excitability. This has been done for an analogous chemical medium using the Oregonator model (Jahnke *et al*, 1988, 1989; Winfree & Jahnke, in press). For heart muscle it is more difficult because the best available electrophysiological equations (based on the approximation of myocardium to a single continuous uniformly anisotropic homogeneous membrane) turn out to describe re-entry little better than the FitzHugh–Nagumo caricature of 28 years ago. That might partly be because cardiac tissue is not a single continuous uniformly anisotropic homogeneous membrane. So for the moment the work proceeds by interaction of qualitative and topological reasoning with laboratory experiments for quantitation.

The corresponding design for a three-dimensional experiment equivalent to sections 4 and 5 is suggested in Winfree (1987). The feasibility of creating vortex filaments in three dimensions has already been shown in artificially paced canine ventricle (Chen *et al.*, 1988; Frazier *et al.*, in press). The arrangement of gradients in that experiment oriented the vortex filaments transmurally. Turning the prestimulus phase gradient 90°, as in normal endocardial activation, would also turn the vortex filaments 90°. They would then be intramural, and in fact should constitute a closed ring as in Fig. 8(c, right) if the stimulus field has cylindrical symmetry. This design is elaborated in Winfree (1989*a*).

All the foregoing is about ventricular tachycardia, not directly about fibrillation. Tachycardia commonly degenerates spontaneously to fibrillation but the process is not understood. It is tempting to imagine that fibrillation may someday be understood in terms of re-entrant vortices, perhaps much closer together and smaller than those studied above. This perspective seems incompatible with the inference of Chen *et al.* (1986*a*,*b*, in press) from defibrillation attempts observed through AC-coupled bipolar electrodes several mm apart, that an unsuccessful defibrillating shock eliminates all activation fronts throughout the three-dimensional bulk of the ventricles, thus eliminating the possibility of reentry, yet fibrillation resumes after a strictly quiescent interval of 18–64 msec. Curiously, it resumes in a nearly synchronous way with a period indistinguishable from that of vortex reentry. These crucial experiments deserve the attention of theorists, and might also bear repeating with improved technology.

William Skaggs (graduate student in Applied Mathematics, University of Arizona) executed the FHN computations on the John von Neumann Supercomputer Center's Cyber 205 in late 1986; William Guilford (graduate student in Physiology, University of Arizona) programmed the first moving display of Shibata *et al.* (1988) data in early 1987; hand-holding and an errata sheet from Michael Guevara (McGill University Medical School) were essential in getting the DiFrancesco–Noble model correctly programmed; Raymond Ideker (Basic Arrhythmias Laboratory, Duke University Medical School) exchanged ideas and data during his sabbatical visits to Tucson in 1986–1987. This material was gathered for presentation at a symposium of the University of Napoli in Capri, May 1987; at the Gordon Research Conference on Theoretical Biology June 1988; at the Canadian Society of Electrophysiologists meeting June 1988; and at NATO Advanced Workshop on Cell-Cell Interactions October 1988. Francis Witkowski, M.D. (University of Alberta Medical School), James McClelland,

M.D. (Oregon Health Science University), Marc Courtemanche (graduate student in Applied Mathematics, University of Arizona), and Chris Henze (graduate student in Ecology and Evolutionary Biology, University of Arizona) made many crucial corrections while struggling valiantly to make the written version readable. Leon Glass and Michael Guevara (McGill University Medical School) provided more challenging critiques than in the total of all my prior journal submissions; the text doubled in length in the course of addressing the queries of successive referees. Research support came from the U.S. National Science Foundation (Cellular Physiology), the John von Neumann Supercomputer Center, and the John D. and Catherine T. MacArthur Foundation.

REFERENCES

AKIYAMA, T. (1981). *Am. J. Physiol.* **240,** H465-H471.

ALLESSIE, M. A. (1989). In: *Theoretical Models for Cell to Cell Signalling.* (Goldbeter, A., ed.) N.Y.: Academic Press.

ALLESSIE, M. A., BONKE, F. I. M. & SCHOPMAN, F. J. G. (1976). *Circ. Res.* **39,** 168-177.

ALLESSIE, M. A., BONKE, F. I. M. & SCHOPMAN, F. J. G. (1977). *Circ. Res.* **41,** 9-18.

BEELER, G. W. & REUTER, H. (1977). *J. Physiol.* **268,** 177-210.

BERNE, R. M. & LEVY, M. N. (1983). *Cardiovascular Physiology.* (4th ed.) pp. 452, 459-460. St Louis: C. V. Mosby.

BOINEAU, J., SCHUESSLER, R., MOONEY, C., MILLER, C., WYLDS, A., HUDSON, R., BORREMANS, J. & BROCKUS, J. (1980). Natural and Evoked Atrial Flutter Due to Circus Movement in Dogs. *Am. J. Cardiol.* **45,** 1167-1181.

BROOKS, C., HOFFMAN, B., SUCKLING, E. & ORIAS, O. (1955). *The Excitability of the Heart.* New York: Grune and Stratton.

CARDINAL, R., VERMEULEN, M., SHENASA, M., ROBERGE, F., PAGE, P., HELIE, F. & SAVARD, P. (1988). *Circulation* **77(5)** 1162-1176.

CHEN, P. S., SHIBATA, N., DIXON, E. G., MARTIN, R. O. & IDEKER, R. E. (1986*a*). *Circulation* **73(5),** 1022-1028.

CHEN, P. S., SHIBATA, N., DIXON, E. G., WOLF, P., DANIELY, N., SWEENEY, M., SMITH, W. & IDEKER, R. E. (1986*b*). *J. Clin. Invest.* **77,** 810-823.

CHEN, P. S., WOLF, P. D., BOWLING, S. D., DANIELEY, N. D., SMITH, W. M. & IDEKER, R. E. (1989). #3068 (in press).

CHEN, P. S., WOLF, P. D., DIXON, E. G., DANIELEY, N. D., FRAZIER, D. W., SMITH, W. M. & IDEKER, R. E. (1988). *Circ. Res.* **62,** 1191-1209.

DIFRANCESCO, D. & NOBLE, D. (1984). *Phil. Trans. R. Soc. B* **307,** 353-398.

DILLON, S., ALLESSIE, M. A., URSELL, P. C. & WIT, A. L. (1988). *Circ. Res.* **63,** 182-206.

DILLON, S. & WIT, A. L. (1988). *IEEE Eng. Biol. Soc.* **10,** 215-216.

DOWNAR, E., PARSON, I. D., MICKLEBOROUGH, L. L., YAO, L. C., CAMERON, D. A. & WAXMAN. M. B. (1984). *J. Am. Coll. Card.* **4(4),** 703-714.

DOWNAR, E., HARRIS, L., MICKELBOROUGH, L. L., SHAIKH, N. & PARSON, I. D. (1988). *J. Am. Coll. Cardiol.* **11(4)** 783-791.

DROUHARD, J. P. & ROBERGE, F. A. (1982). *IEEE Trans. Biomed. Eng.* **BME-29(7),** 494-502.

EL-SHERIF, N. (1985). In: *Cardiac Electrophysiology and Arrhythmias* (Zipes, D. P. & Jalife, J., eds.) pp. 363-378. Orlando, FL: Grune & Stratton.

EL-SHERIF, N., SMITH, R. A. & EVANS, K. (1981). *Circ. Res.* **49,** 255-265.

EL-SHERIF, N. (1988). Reentry Revisited. *PACE* **11,** 1358-1368.

FABIATO, A., COUMEL, R., GOURGON, R. & SAUMONT, R. (1967). *Arch. Mal. Coeur.* **60(4)** 527-544.

FITZHUGH, R. A. (1960). *J. Gen. Physiol.* **43,** 867-896.

FITZHUGH, R. A. (1961). *Biophys. J.* **1,** 445-466.

FOY, J. L. (1974). *Technical Report No. 166.* Ann Arbor, Michigan: University of Mich. Department of Computer Science.

FRAZIER, D. W., WOLF, P. D., WHARTON, J. M., TANG, A. S. L., SMITH, W. M. & IDEKER, R. E. *J. Clin. Invest.* (in press).

FRAZIER, D. W., WOLF, P. D. & IDEKER, R. E. (1988*b*). *PACE* **11(4),** 482.

FRAZIER, D. W., WOLF, P. D., WHARTON, J. M., TANG, A. S. L., SMITH, W. M. & IDEKER, R. E. *J. Clin. Invest.* (in press).

GARREY, W. E. (1914). *Am. J. Physiol.* **33,** 397-414.

GOLDBERGER, A. L., BHARGAVA, V., WEST, B. J. & MANDELL, A. J. (1986). *Physica* **19D**, 282.
GOLDBERGER, A. L. & RIGNEY, D. R. In: *Dynamics Patterns in Complex Systems* (Kelso, J. A. S., Mandell, A. J. & Schlesinger, M. F., eds.) Singapore: World Scientific Publishers.
GOUGH, W. B., MEHRA, R., RESTIVO, M., ZEILER, R. H. & EL-SHERIF, N. (1985). *Circ. Res.* **57**, 432-442.
GUEVARA, M., SHRIER, A. & GLASS, L. (1986). *Am. J. Physiol.* **251**, H1298-H1305.
GUL'KO, F. B. & PETROV, A. A. (1972). *Biofizika* **17**, 261-270.
HODGKIN, A. L. & HUXLEY, A. F. (1952). *J. Physiol.* **117**, 500-544.
IDEKER, R. E. & SHIBATA, N. (1986). *Proc. Int. Union Physiol. Sci.* **16**, 88.
IDEKER, R. E., FRAZIER, D. W., KRASSOWSKA, W., CHEN, P. S. & WHARTON, J. M. (in press).
IDEKER, R. E., SMITH, W. M., WOLF, P., DANIELEY, N. D. & BARTRAM, F. R. (1987). *PACE* **10**, 281-292.
JAHNKE, W., HENZE, C. & WINFREE, A. T. (1988). *Nature, Lond.* **336**, 662-665.
JAHNKE, W., SKAGGS, W. E. & WINFREE, A. T. (1989). *J. Phys. Chem.* **93**, 740-749.
JANSE, M. J., VAN DER STEEN, A. B. M., VAN DAM, R. TH. & DURRER, D. (1969). *Circ. Res.* **24**, 251-262.
JOYNER, R. W., RAMON, F. & MOORE, J. W. (1975). *Circ. Res.* **36**, 614-661.
KADISH, A., SHINNAR, M., MOORE, E. N., LEVINE, J. H., BALKE, C. W. & SPEAR, J. F. (1988). Interaction of Fiber Orientation and Direction of Impulse Propagation with Anatomic Barriers in Anisotropic Canine Myocardium. *Circulation* **78**, 1478-1494.
KEENER, J. P. (1986). *SIAM J. Appl. Ma.* **46(6)**, 1039-1056.
KEENER, J. P. & TYSON, J. J. (1986). *Physica* **21D**, 307-324.
LESIGNE, C., LEVY, B., SAUMONT, R., BIRKUI, P., BARDOU, A. & RUBIN, B. (1976). *Med. Biol. Eng.* **14**, 617-622.
MCKEAN, H. P., JR. (1970). *Adv. Math.* **4**, 209-223.
MEHRA, R. (1984). *IEEE Eng. Med. Biol.* **June**, 34-35.
MEHRA, R., ZEILER, R. H., GOUGH, W. B. & EL-SHERIF, N. (1983). *Circ.* **67(1)**, 11-24.
MINES, G. R. (1914). *Trans. R. Soc. Can.* **4**, 43-53.
MOE, G. K. (1962). *Arch. Int. Pharmacodyn.* **140**, 183-188.
MOE, G. K., HARRIS, A. S. & WIGGERS, C. J. (1941). *Am. J. Physiol.* **134**, 473-492.
MOE, G. K., RHEINBOLDT, W. C. & ABILDSKOV, J. A. (1964). *Am. Heart J.* **67**, 200-220.
MOGUL, D. J., THAKOR, N. V., MCCULLOUGH, J. R., MYERS, G. A., TENEICK, R. E. & SINGER, D. H. (1984). In: *Computers in Cardiology* pp. 159-161. Long Beach, CA: IEEE Computer Society.
MOORE, J. W. & RAMON, F. (1974) *J. theor. Biol.* **45**, 249-273.
PERTSOV, A. M., ERMAKOVA, E. A. & PANFILOV, A. V. (1984). *Physica* **14D(1)**, 117-124.
PLONSEY, R. & BARR, R. C. (1984). *Biophys. J.* **45**, 557-571.
RANDALL, J. E. (1980). Cardiac Action Potentials (Ch. 13). In: *Microcomputers and Physiological Simulation.* Reading, MA: Addison-Wesley.
REINER, V. S. & ANTZELEVITCH, C. (1985). *Am. J. Physiol.* **249**, H1143-H1153.
RUELLE, D. (1980). *Mathe. Intell.* **2**, 126.
SCOTT, A. C. (1977). *Neurophysics.* N.Y.: Wiley.
SALAMA, G., LOMBARDI, R. & ELSON, J. (1987). *Am. J. Physiol.* **252**, H384-H394.
SHCHERBUNOV, A. I., KUKUSHKIN, N. I. & SAKSON, M.Y. (1973). *Biofizika* **18**, 519-525.
SHIBATA, N., CHEN, P. S., DIXON, E. G., WOLF, P. D., DANIELEY, N. D., SMITH, W. M. & IDEKER, R. E. (1988). *Am. J. Physiol.* **255**, H891-H909.
SMITH, J. M. & COHEN, R. J. (1984). *Proc. natn. Acad. Sci. U.S.A.* **81**, 233.
STEINHAUS, B. M., SPITZER, K. W., BURGESS, M. J. & ABILDSKOV, J. A. (1986). *Computers in Cardiology.* pp. 421-426. Long Beach, CA: IEEE Computer Society.
SWENNE, C., BOSKER, H. A. & VAN HEMEL, N. M. (1986). *Computers in Cardiology.* pp. 445-448. Long Beach, CA: IEEE Computer Society.
TYSON, J. J. & FIFE, P. C. (1980). *J. Chem. Phys.* **73(5)**, 2224-2237.
TYSON, J. J. & KEENER, J. P. (1987). *Physica D*, **29D(1-2)**, 215-222.
TYSON, J. J. & KEENER, J. P. (1988). *Physica D*, **32**, 327-361.
TYSON, J. J. & MANORANJAN, V. S. (1984). In: *Non-equilibrium Dynamics in Chemical Systems.* (Vidal, C. & Pacault, A., eds.) Berlin: Springer-Verlag.
VAN CAPELLE, F. J. & DURRER, D. (1980). *Circ. Res.* **47**, 454-466.
VAN CAPELLE, F. J. & ALLESSIE, M. A. In: *Theoretical Models for Cell to Cell Signalling.* (Goldbeter, A., ed.) N.Y.: Academic Press (in press).
WINFREE, A. T. (1967). *J. theor. Biol.* **16**, 15-42.
WINFREE, A. T. (1973). In: *Advances in Biological and Medical Physics* (Lawrence, J. H., ed.) pp. 115-136. New York: Academic Press.
WINFREE, A. T. (1974*a*). *Scient. Am.* **230(6)**, 82-95.

WINFREE, A. T. (1974*b*). *SIAM/AMS Proc.* **8**, 13-31.
WINFREE, A. T. (1978). *Prog. Theor. Chem.* 4,1-51.
WINFREE, A. T. (1980). *The Geometry of Biological Time.* New York: Springer-Verlag.
WINFREE, A. T. (1982). In: *Cardiac Rate and Rhythm* (Bouman, L. N., Jongsma, H. J. & Nijhoff, M., eds) pp. 447-472. The Hague.
WINFREE, A. T. (1983). *Scient. Am.* **248(5)**, 144-161.
WINFREE, A. T. (1985). In: *Oscillations and Traveling Waves in Chemical Systems* (Field, R. & Burger, M., eds.) pp. 441-472. New York: Wiley.
WINFREE, A. T. (1986*a*). *The Timing of Biological Clocks.* New York, N.Y.: Scientific American Books.
WINFREE, A. T. (1986*b*). *Proc. Int. Union Physiol. Sci.* **16**, 287.
WINFREE, A. T. (1987). *When Time Breaks Down.* Princeton: Princeton University Press.
WINFREE, A. T. (1989*a*). *Cell to Bedside.* In: *Cardiac Electrophysiology* (Zipes, D. P. & Jalife, J., eds) San Diego: W. B. Saunders Co.
WINFREE, A. T. (1989*b*). In: *Theoretical Models for Cell to Cell Signalling.* (Goldbeter, A., ed.) New York: Academic Press.
WINFREE, A. T. & GUILFORD, W. (1988). In: *Biomathematics and Related Computational Problems* (Riccardi, L. M., ed.) pp. 697-716. Kluwer Academic Publishers.
WINFREE, A. T. & JAHNKE, W. *J. Phys. Chem.* (in press).
WINFREE, A. T. & STROGATZ, S. H. (1983). *Physica* **8D**, 35-49.
WIT, A. L., ALLESSIE, M. A., BONKE, F. I. M., LAMMERS, W., SMEETS, J. & FEBIFKUI, J. J. (1982). *Am. J. Card.* **49**, 166-185.
WIT, A. L. & CRANEFIELD, P. F. (1978) *Am. J. Physiol.* **235(1)**, H1-H17.
WITKOWSKI, F. X. & PENKOSKE, P. A. (1988*a*). *IEEE EMBS conference* (in press).
WITKOWSKI, F. X. & PENKOSKE, P. A. (1988*b*). *J Electrocard.* **21(3)**, 273-282.
ZYKOV, V. S. (1984). *Simulation of Wave Processes in Excitable Media.* Moscow: Nauka [also in 1988 translation (Winfree, A. T., ed.) Manchester University Press].
ZYKOV, V. S. (1986). *Biofizika* **31(5)**, 862-865.
ZYKOV, V. S. (1987). *Biofizika* **32(2)**, 337-340.

APPENDIX

Historical Background

Until the early 1970's the theory of reentry in two- or three-dimensional media required a physical or at least functional hole in the medium. This was independently corrected in the Russian (Gul'ko & Petrov, 1972; Shcherbunov *et al.*, 1973) and English (Winfree, 1973, 1974*a,b*, 1978) literatures, with consequences for cardiac electrophysiology that are only now fully coming to light (e.g. Zykov, 1984). Cutting across the Russian/English strands of this literature are the electrophysiology/physical chemistry strands. They differ greatly in jargon but little in principles of rotor behavior. The main difference is that the chemical systems involve diffusion of all local variables, whereas the electrophysiological membranes admit diffusion of only one local variable (the membrane potential, diffusion of other variables being limited by the diffusion coefficients of proteins in the lipid membrane and conventionally set to zero). But I have never observed a major qualitative change in reentrant wave behavior in chemically excitable media (equal diffusion) when the "recovery" variable is made immobile either computationally or in the laboratory.

The "local interpretation in terms of membrane mechanism" (section 3.2) was 3.2) was developed in Winfree (1974*a,b*, 1978, 1980) in the context of chemically excitable media, and reviewed in Winfree (1987, appendix) in the present context. Topological notions about oscillator phase resetting (Winfree 1982, 1983, 1987) constitute a conceptually simpler analogy, replacing the two variables of Winfree (1974*a,b*, 1978) by just one: phase as a measure of state around a loop trajectory.

The process here described as inducing reentry in excitable media does so in the same way (hanging the medium's image over the usual loop trajectory) whether or not the medium self-excites spontaneously. But it is much easier to describe in the oscillatory case, by reference to the angular measure, "phase", around the loop.

Any stably rhythmic system can have its phase reset by a fleeting stimulus that touches its mechanism—for example by an electric impulse in the case of heart muscle. If the measured dependence of the reset phase on the timing of the stimulus can be fairly represented as a continuous curve, and if that curve's mean slope is not 1, then by a proven mathematical theorem there must exist a critical phase in the cycle when a smaller stimulus of critical strength must result in unpredictable resetting or failure to return to the normal cycle (Winfree 1980, 1986*a*, 1987): i.e. dysrhythmia. This is true of any such non-linear dynamical system no matter how complicated, so it might be true of the heart considered as a whole (Winfree, 1980, 1982, 1983). If so, it provides the seed of an interpretation of the *vulnerable period*, that interval in the cardiac cyle when dysrhythmia leading to fibrillation can be easily induced by a tiny stimulus. Thus if the heart were entirely composed of sinoatrial node tissue characterized by continuous phase-resetting curves, then the topological theorem would require the existence of arrhythmias evoked by stimulation of critical size at a critical time. Their geographic interpretation involves waves rotating about phase singularities (Winfree, 1982, 1983, 1987). The principles involved throughout this paper could then have strict analogies to mathematical theorems.

As it happens, they do not, because the heart is composed of distinct tissues and the ventricular myocardium in particular does not spontaneously repeat its loop in state space. (Also it is not yet clear that the resetting curves of cardiac oscillators are mathematically continuous; they are not, for example, in spontaneously beating balls of tissue-cultured embryonic chick ventricular cells, Guevara *et al.*, 1986.) Nonetheless, its dynamics within each loop bears a strong analogy to the dynamics of each cycle of an oscillatory membrane's mechanism. The mechanisms of stimulation and reset of timing are sufficiently similar that vortex initiation in either medium occurs by essentially the same process, as shown in numerical experiments and in the laboratory using analogous chemically excitable and/or oscillatory media. The main principle in all cases is the creation of transverse gradients spanning the excitation-recovery loop [Figs 2(c), 6(c)] in a large enough area, as demonstrated numerically in Winfree (1974*a*,*b*), chemically in Winfree (1985), again numerically here (Figs 12 and 14), and in recent physiological experiments (Shibata *et al.*, 1988, Frazier *et al.*, 1989).

However the *phase* of evoked rotation is one of the quantitative particulars that depend sensitively on quantitative specifications of the dynamics. Winfree (1987) illustrated the topological concepts using an analytical model based on sinusoidal limit-cycle oscillation (similar to the Reiner & Antzelevitch, 1985, model of sinoatrial node membrane featured in that book) to maximize simplicity of diagrams. Those models are faithful to little about *myocardial* membrane dynamics beyond the pursuit of a loop trajectory in state space. The sinusoidal model completely lacks anything like the separator trajectory, which occurs at about 120° prior to maximum depolari-

zation, measured from the middle of the excitation-recovery loop in Fig. 2. These two regions of state space are about 1/3 period apart along the sinusoidal limit cycle's trajectories, but almost adjacent in time in the excitable model: transgressing the separator is tantamount to achieving maximum depolarization very shortly later. Figure 6.2 of Winfree (1987) used the isochron of maximum depolarization as the criterion of "wavefront" in the smooth limit-cycle model. This locus falls geographically on $S > S^*$ side of the T^* isochron. But using a locus more appropriate for *excitable* local kinetics, an isochron 120° anticlockwise in state space (where the separator would be, were the trajectories tailored to more resemble an excitable medium as in Fig. 2), the post-shock wavefront would have fallen about 1/3 cycle ahead, as in the computer simulations and laboratory experiments with *excitable* media described in the main text of this paper. The best way to approach these questions is to abandon analytically solvable models and topological theorems, resorting instead to laboratory experiments with real myocardium and chemically-excitable analogs, and to numerical experiments with more realistic models.

The FitzHugh–Nagumo Two-variable Model

The FitzHugh-Nagumo membrane model (FitzHugh, 1961) was used in the form

$$dA/dt = (A - B - A^3/3)/\varepsilon + D(d^2A/dx^2 + d^2A/dy^2)$$

$$dB/dt = \varepsilon(A - \gamma B + \beta)$$

with parameters $\beta = 0.7$, $\gamma = 0{\cdot}8$ as in the original publication, but epsilon decreased from FitzHugh's 0·333 to 0·2 to enable propagation. (With parameters β and γ as given, this medium is "excitable" in the sense of sustaining propagation of a pulse only for epsilon less than about 0·3; FitzHugh apparently had done only computations of space-clamped excitability by 1961.) The variable A represents membrane potential and B represents a recovery process. High values of A and/or of B contribute (for different physical reasons) to refractoriness. The phase portrait of this local kinetics (i.e. with $D = 0$ or no gradients) is drawn in Winfree (1987, appendix) and in FitzHugh (1961); it looks very much like Fig. 2.

A and B can be interpreted as certain combinations of the four variables of the Hodgkin-Huxley equations (FitzHugh, 1960, 1961; Scott, 1977) but it is not necessary to do so at this stage; the translation is different for different membranes. The trajectories in Fig. 2 differ in many particulars from those of mammalian ventricular membrane; for example they show an overshooting repolarization ("early afterhyperpolarization") prior to termination of the recovery process (lower right corner). When a quantitatively reliable electrophysiological model of ventricular myocardium becomes available it will replace this caricature; meanwhile this discussion is limited to features that I expect are common to both versions.

Parameter D has the dimension of space units^2/time unit, like a chemical diffusion coefficient. Numerically, it depends on the choice of units, here chosen to make D numerically 1. In physiological units, it is proportional to the reciprocal product of

tissue resistivity and capacitance and a surface/volume ratio characterizing tissue architecture (Joyner *et al.*, 1975; Steinhaus *et al.*, 1986). In the discretized computation the Laplacian is estimated as a second difference of A values at adjacent grid points:

$$D(\mathrm{d}^2A/\mathrm{d}x^2+\mathrm{d}^2A/\mathrm{d}y^2)=(D/h^2)[(A_N-A_c)+(A_E-A_c)+(A_S-A_c)+(A_W-A_c)]$$

where subscripts N, E, S, W and c indicate north, east, south, west and center. Taking D = 1 space unit^2/time unit, the square root of coefficient D/h^2 is proportional to the number of sample points per linear space unit. Coefficient $D/h^2 =$ 6·25(time units^{-1}) was found to be more than sufficient for reliable computation with the FitzHugh–Nagumo cable equation; sample points are then 0·4 space unit apart. If this coefficient is made much larger, then the sample points are closer together so the whole medium (represented by a fixed number of sample points) becomes smaller; ultimately, the vortex core does not fit and its rotor goes unstable. If the coefficient is made much smaller then sample points are too far apart (and the medium is correspondingly larger) or are too nearly uncoupled electrically to maintain the continuous spatial gradients of activity that constitute a rotor.

Time and space were then scaled so that solitary action potentials propagate at 0·5 mm/msec and rotors have 100–120 msec period: the unit of time is 10 msec, the unit of space is 2·5 mm, and sample points are 1 mm apart. Computations were updated at intervals $\mathrm{d}t = 0{\cdot}02$ time units, corresponding to 0·2 msec. The abstract quantity A (rising from −1·2 to 2·0 during excitation) is scaled to represent membrane potential (−84 to +22 mV) by $V_m = 33A - 44$, and B (ranging about −1 to 1) is renamed as $R = (B+1)/2$ to range about 0 to 1. The rest state lies at the intersection of the linear $\mathrm{d}B/\mathrm{d}t = 0$ nullcline with the cubic nullcline $\mathrm{d}A/\mathrm{d}t = 0$ at $A = -1{\cdot}2$, $B = -0{\cdot}62$, with threshold (the "separator" trajectory just above the middle branch of the cubic nullcline) 17 mV above it at $A = -0.7$ (cf. 24 mV nominal threshold for real myocardium). A slight adjustment of parameters makes the model spontaneously oscillatory without upsetting the processes described here. Similar slight adjustments to make it incapable of sustaining a traveling pulse (e.g. raising ε above about 0·3) leave the initiation of rotors unaltered, but they become unstable.

Computations on a 75 × 75 array (mirror-duplicated to 75 × 150) were started with the array uniformly at equilibrium. Then one edge was depolarized by elevating A above threshold, and the resulting wavefront was allowed to cross the rectangle repeatedly (by temporarily joining opposite edges) until the propagating action potential stabilized.

The stimulus was applied as an instantaneous offset of A, independent of A or B (as though injecting a current impulse with membrane resistivity constant). Its local strength was a monotone decreasing function of radius (r, in mm) from the electrode, supposing that the total current, I, is the same through any ring around the electrode. Then the local current density $j = I/(2\pi r)$. The effective stimulus S (the greatest depolarization imposed upon any patch of membrane in the tangle of diversely oriented membranes constituting the cellular medium) is supposed proportional to j. However S should not exceed the physiological range as r approaches

zero. These requirements are roughly satisfied by

$$S = 0{\cdot}8 * 33\ \text{mV}/\sqrt{\{0{\cdot}2 + [r(\text{in mm})/(15 * 2{\cdot}5\ \text{mm})]^2\}}$$

so $S = 66$ mV under the electrode and $S = 11{\cdot}6$ mV at the corners of the rectangle (with excitation threshold $S = 17$ mV).

The Beeler–Reuter Many-variable Model

The FitzHugh–Nagumo model lacks most of the variables present in a complete electrophysiological dissection of the ionic currents. A two-variable model is the simplest that can reliably capture the essentials of excitability and recovery, and its scales of time and space must be adjusted to conform to those of the medium simulated. The Beeler–Reuter model (Beeler & Reuter, 1977; Randall, 1980) contains much more realistic physiological detail: four ionic currents besides membrane potential, requiring altogether eight differential equations. There are no "disposable" parameters: all are measured quantities. Our numerical methods of 1986–1987 follow Randall (1980), using the modified Euler method of Moore & Ramon (1974) with time step $dt = 0{\cdot}1$ msec. The complicated exponential polynomial terms are evaluated at the outset and tabulated for interpolation during the simulation. The calcium potential E_{si} is not fixed, since we found (contrary to Drouhard & Roberge, 1982) that taking such a shortcut does unacceptably alter the computational results. The calculation is extended (still using explicit Euler method with discrete Laplacian, not using the implicit method preferred by Steinhaus *et al.*, 1986) from a single cell to a square of 200×200 connected cells to check the existence and stability of two-dimensional vortex reentry. The spatial grid was coarse (to save computer time), using diffusion coefficient (of the electric potential) $D/h^2 = 0{\cdot}3$ msec^{-1} in most runs. (D is the coefficient of the Laplacian coupling term as in the FitzHugh model above, numerically = 1 space unit^2/time unit; h is the simulated spacing between grid points, in space units.) An exploration of one-dimensional propagation speed as a function of combinations of $0{\cdot}025 \leq dt \leq 0{\cdot}4$ time unit and $0{\cdot}3 \leq D/h^2 \leq 2{\cdot}0$ (alias $0{\cdot}7 \leq h \leq 1{\cdot}8$ space units) suggests an asymptotic speed (as h and dt become very small) of 1·5 space units per time unit. If this is to represent 0·5 mm/msec, then since the Beeler–Reuter equation's time unit is 1 msec, 1 space unit must be 1/3 mm. At $D = 1/h^2 = 0{\cdot}3$ msec^{-1} as in most of these numerical experiments, $h = 1{\cdot}82$ space units = 0·6 mm as in Steinhaus *et al.* (1986), and the activation thus coarsely simulated propagates at only about 60% of the extrapolated correct speed. This is crude, but adequate for the limited purposes of this paper; methods have been improved in the interim (Courtemanche & Winfree, unpublished results).

The Beeler–Reuter membrane model has never before been examined for ability to support vortex reentry in two or three dimensions. When we confirmed this ability it unfortunately also turned out that quantitative realism is still imperfect, so further investigations were not pursued: the model's vortex period is about twice as long as observed in dogs, and so still requires *ad hoc* adjustment of time and space scales just as the FitzHugh–Nagumo model did. This may be a consequence of the model's unrealistically slow calcium kinetics, if the rotor's period is limited by the refractory

period; or it may be a consequence of deficiencies in the fast opening of sodium channels, if the rotor's period is limited by the dependence of front propagation speed on front curvature in two dimensions; or it may be a consequence of ignoring factors such as accumulation of potassium (typically from 3·5 mM to 7 mM: Mogul *et al.*, 1984) in extracellular clefts during rapid pacing. It seemed possible that there are two kinds of vortex: one with period 200–300 msec involving a relatively normal action potential, and one with calcium plateau aborted, involving only the briefer sodium conductivity pulse. We observed such waves stably circulating with period near 120 msec on one-dimensional rings but did not obtain stable rotors of the same kind during the limited and coarse simulations of 1986–7, except by blocking the calcium channels. These questions require investigation in the Beeler-Reuter model and comparative investigation in a more realistic adaptation of the DiFrancesco–Noble model to myocardium.

The use of models implicating more than two state variables raises a fundamental question about the basic concept advocated in this paper: that re-entry is equivalent to mapping the two-dimensional or three-dimensional medium to state space so that its image spans the excitation-recovery loop. What can this mean if the state space has more dimensions than the physical medium? A two-dimensional medium's image might "span" the loop when viewed from one perspective in a three-dimensional state space, but not span it as viewed from another perspective. The answer is that this "viewing" must be done along trajectories in state space, and can be so done only if motion along those trajectories is swift compared to the motions induced by coupling to neighboring cells (as it is if the gradients of local state are sufficiently shallow). In the case of spontaneously oscillating local kinetics, a topological theorem then provides the wanted criterion: the image spans the limit cycle if and only if "Type 0 phase resetting" is measured when the stimulus is applied at maximum strength to the space-clamped tissue (Winfree, 1980). The close analogy of mechanism, many numerical simulations, and some chemical experiments (but no theorem) suggests that similar behavior should follow in media with three or more state variables whose parameters have been altered to suppress spontaneous oscillation. The "Type 0" criterion might still be used by adjusting the parameters of such media for spontaneous oscillation during the test.